APPENDIX D: CHARACTERIZATION MEASUREMENTS

This appendix provides a description of measurement setup and signal characterization measurements that complement those in Section 3.

D.1. Measurement Setup

Interference signals were measured under optimal conditions at the radio frequency (RF) output of the vector signal generator (VSG) as described in Figure D-1. The VSG was set up with the procedures described in Appendix B of Part 1 [6]. Measurements at RF were made with the vector signal analyzer (VSA) and digital oscilloscope (DO).

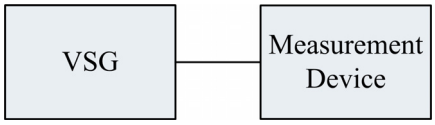

Figure D-1. Setup for RF signal characterization measurements.

The gated-noise signals, GN-02 – GN-17, were simulated by applying different gating signals to the continuous-noise signal, GN-01. This ensured that voltages of all signals were identical when gated on. Gated-noise signals, generated in hardware with the setup described by Figure C-2 in Part 1, were also measured to verify corresponding VSG-generated signals. Characteristics of the hardware-generated signals matched those of the VSG-generated signals and therefore are not included in this report.

For VSA characterization measurements at RF, the VSG output level was set to -28.19 dBm for GN-01 through GN-17 and -27.17 dBm for GN(MB)-01 through GN(MB)-09. At these levels, the VSG generated the "continuous" signals, GN-01 and GN(MB)-01, at an average power of approximately -45 dBm in a 36-MHz bandwidth at the output of the cable. This optimally utilized the dynamic range of the VSA as discussed in Appendix E of Part 1. VSA instrument settings are summarized in Table D-1.

Table D-1. RF VSA Measurement Settings

Post-Processing Bandwidths (MHz)	Span (MHz)	Number of Samples	Center Frequency (MHz)	Input Range (dBm)
36, 19.51, 10 1 0.1	36 4.5 0.5625	> 360,000 > 450,000 > 562,500	3820	-30

DO measurements at the maximum sample rate, i.e., 20 GSps, provided real time-domain representations of RF signals. DO measurements were made with the VSG output level set to a higher value, i.e., 0 dBm, to compensate for low DO sensitivity at the maximum sample rate.

Interference signals were measured under TOV operational conditions at the IF output of the low-noise block downconverter (LNB) with the setup described in Figure 20 of Part 1. The simplified block diagram of those components that affect the IF signal characterization measurements are shown in Figure D-2. Bandpass filter BPF1 has a 1-dB bandwidth equal to 40 MHz. The VSG output level was set to INR_{TOV}. Measurements at IF were made with the VSA only. VSA settings for IF measurements were the same as those used for RF measurements described in Table D-1, except the center frequency was set to 1330 MHz.

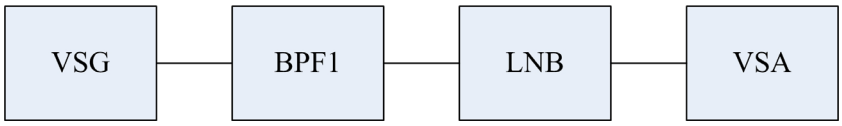

Figure D-2. Simplified setup for IF signal characterization measurements.

D.2. Results

This subsection provides amplitude statistics and time series of the gated-noise signals. Odd numbered plots in Figures D-3 – D-54 provide RF measurement results organized as:

(a) Real time series measured with DO and amplitude time series measured with the VSA and band-limited to B_{DTV} = 19.51 MHz.
(b) *APD*s measured with a VSA and band-limited to 36, 10, 1, and 0.1 MHz as well as B_{DTV}.

Even numbered plots in Figures D-3 – D-54 provide IF measurement results organized as:

(a) Amplitude time series measured with the VSA and band-limited to B_{DTV}.
(b) *APD*s measured with the VSA and band-limited to B_{DTV}.

Table D-2 provides peak-to-average (*P/A*) values for the gated-noise signals measured at RF and band-limited to various bandwidths in post-measurement processing. The shaded cells highlight signals with Rayleigh-distributed amplitudes. Ultra-wide transmission bandwidth (B_{UWB}) limits for *P/A* were derived in Appendix C.

Table D-3 provides *P/A* values for gated-noise signals measured at IF under TOV operational conditions and band-limited to B_{DTV} in post-measurement processing.

Table D-2. RF *P/A* (dB) of GN and GN(MB) Signals Band-Limited to Different Bandwidths

Type	Index	B_{UWB}	36.0 MHz	B_{DTV}	10.0 MHz	1.0 MHz	0.1 MHz
GN	01	9.6	9.6	9.6	9.8	9.8	9.0
	02	12.3	9.7	9.9	9.5	9.7	9.6
	03	14.9	11.0	9.7	9.8	9.5	8.9
	04	17.5	13.1	11.5	9.4	9.5	10.1
	05	20.1	15.9	14.2	11.7	9.8	9.1
	06	12.3	11.8	12.2	11.2	9.5	9.3
	07	14.9	14.4	14.6	13.9	9.6	9.9
	08	17.5	16.8	17.3	16.5	9.7	9.4
	09	20.1	19.8	19.6	18.9	11.7	9.2
	10	12.3	12.5	12.4	12.5	11.1	10.1
	11	14.9	15.1	15.0	14.8	13.6	9.8
	12	17.5	17.9	17.6	17.6	16.3	9.4
	13	20.1	20.3	20.3	20.0	18.8	11.0
	14	12.3	12.6	12.3	12.2	12.3	10.3
	15	14.9	15.3	15.1	14.8	14.8	14.1
	16	17.5	17.4	17.8	17.9	17.6	15.7
	17	20.1	19.9	20.1	20.0	19.9	16.4
GN (MB)	01	10.6	10.5	10.5	10.1	9.6	9.7
	02	14.8	14.4	14.7	14.6	9.8	9.5
	03	14.8	14.7	14.6	14.5	11.6	9.5
	04	18.0	17.5	18.0	17.6	12.7	9.7
	05	18.0	17.6	17.9	17.5	14.7	9.5
	06	18.0	17.6	17.8	17.6	16.5	10.6
	07	20.3	20.1	20.2	19.7	15.0	9.4
	08	20.3	20.0	20.1	19.8	16.8	9.0
	09	20.3	20.1	19.9	19.5	19.0	15.0

*Shaded cells highlight Rayleigh-amplitude statistics.

Table D-3. IF *P/A* (dB) of GN and GN(MB) Signals at INR_{TOV} and Band-Limited to B_{DTV}

Type	Index	*SNR* ≈ 9 dB	*SNR* ≈ 12 dB	*SNR* ≈ 15 dB
GN	01	9.6	9.6	9.4
	02	9.8	9.8	9.9
	03	9.6	9.5	9.5
	04	10.4	11.1	11.1
	05	12.0	13.2	13.6
	06	10.8	11.1	11.7
	07	12.1	13.2	13.8
	08	14.1	15.2	16.4
	09	16.1	17.8	18.8
	10	11.2	11.4	11.8
	11	11.9	13.1	13.7
	12	13.0	14.6	15.8
	13	13.5	16.2	17.5
	14	10.7	11.5	12.0
	15	11.4	12.8	13.6
	16	12.0	13.8	15.3
	17	11.9	14.3	16.6
GN (MB)	01	10.2	10.2	10.3
	02	12.1	13.3	14.3
	03	12.0	13.4	13.9
	04	14.0	16.2	16.7
	05	13.5	15.4	16.4
	06	12.6	14.6	15.8
	07	15.0	17.8	18.7
	08	14.3	16.5	17.9
	09	12.7	15.2	17.4

*Shaded cells highlight Rayleigh-amplitude statistics.

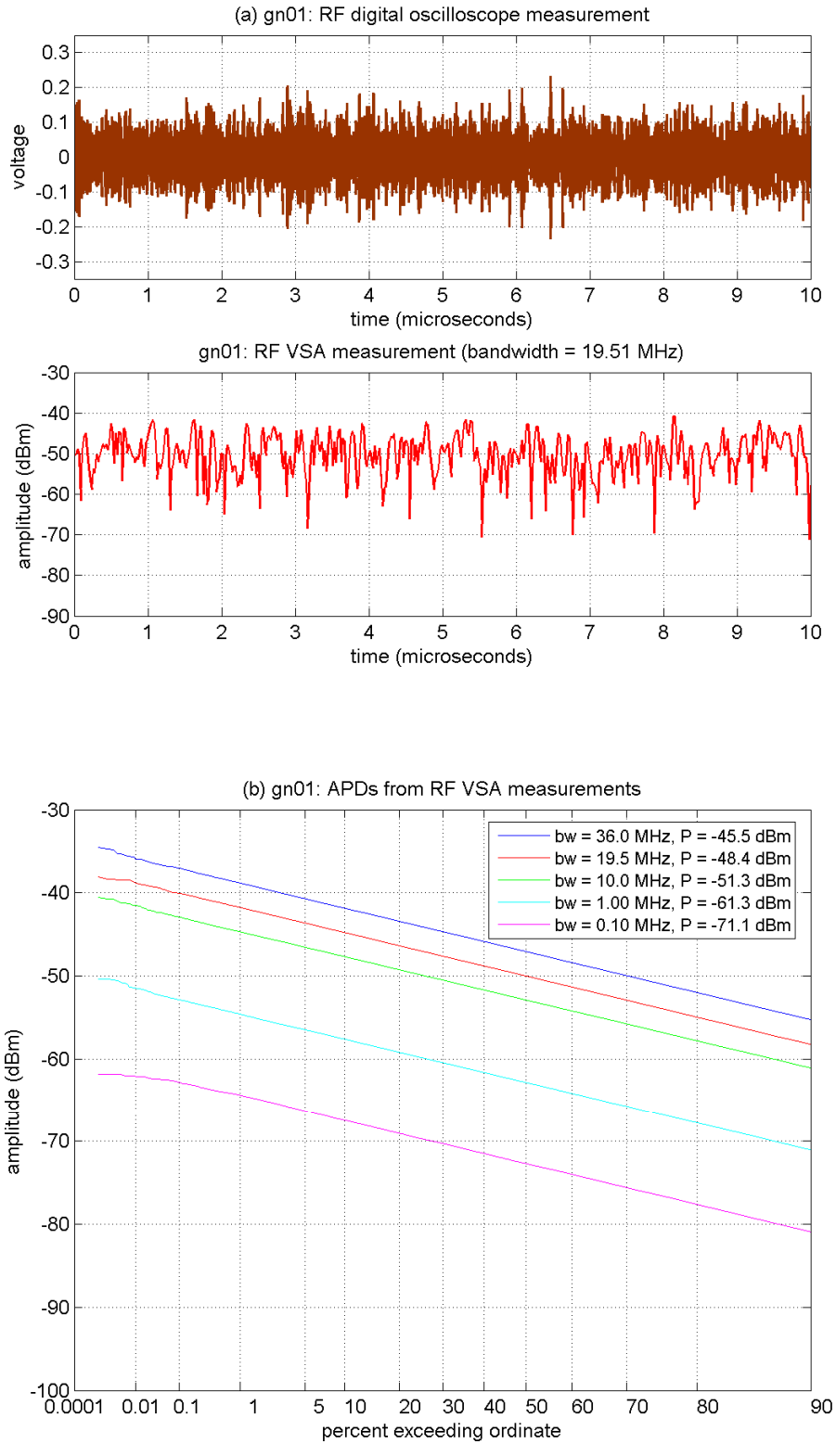

Figure D-3. RF measurements of GN-01, Gaussian noise.

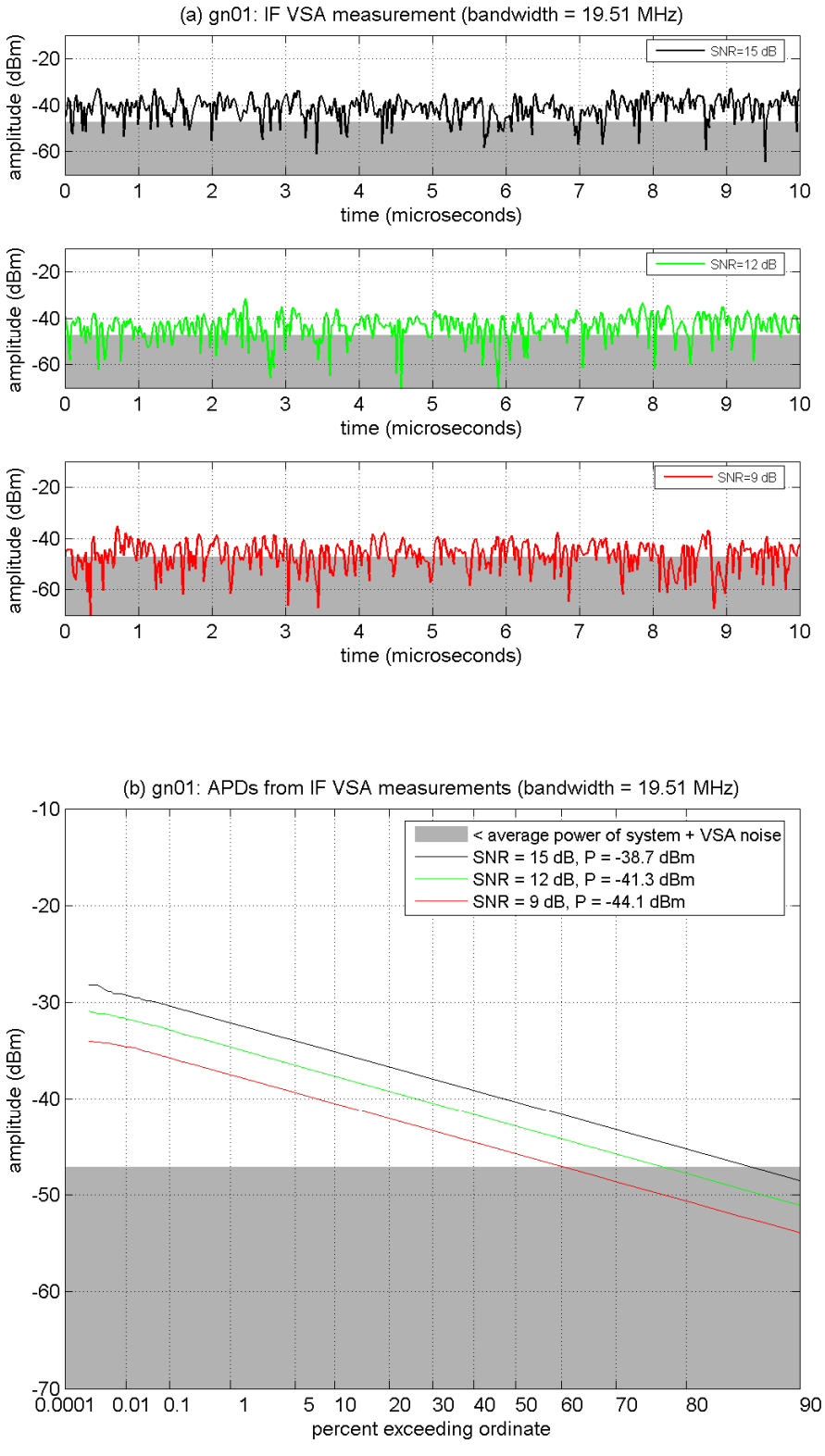

Figure D-4. IF measurements of GN-01 at INR_{TOV}.

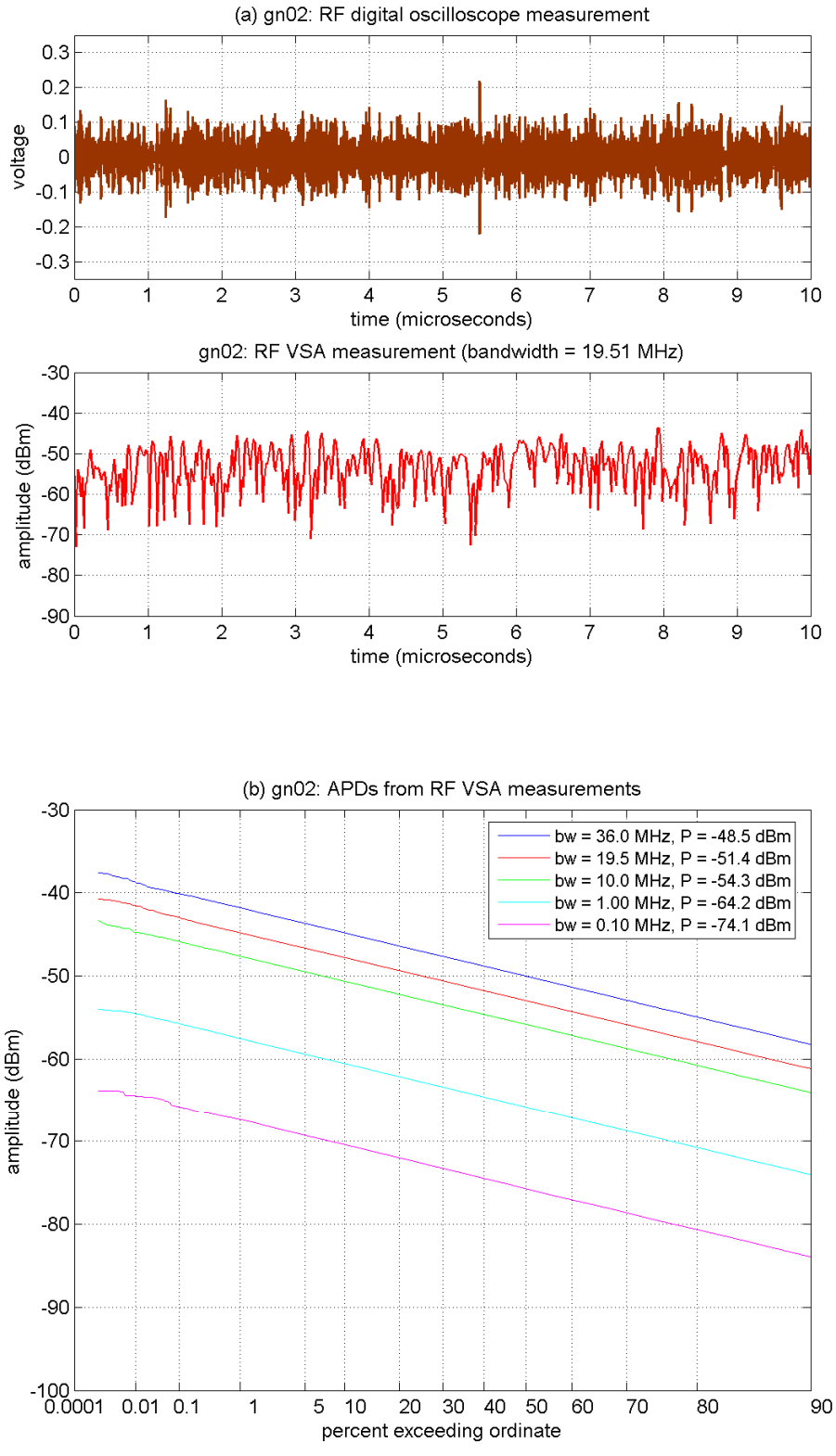

Figure D-5. RF measurements of GN-02 (τ_{on} = 10 ns, ζ = 0.5000).

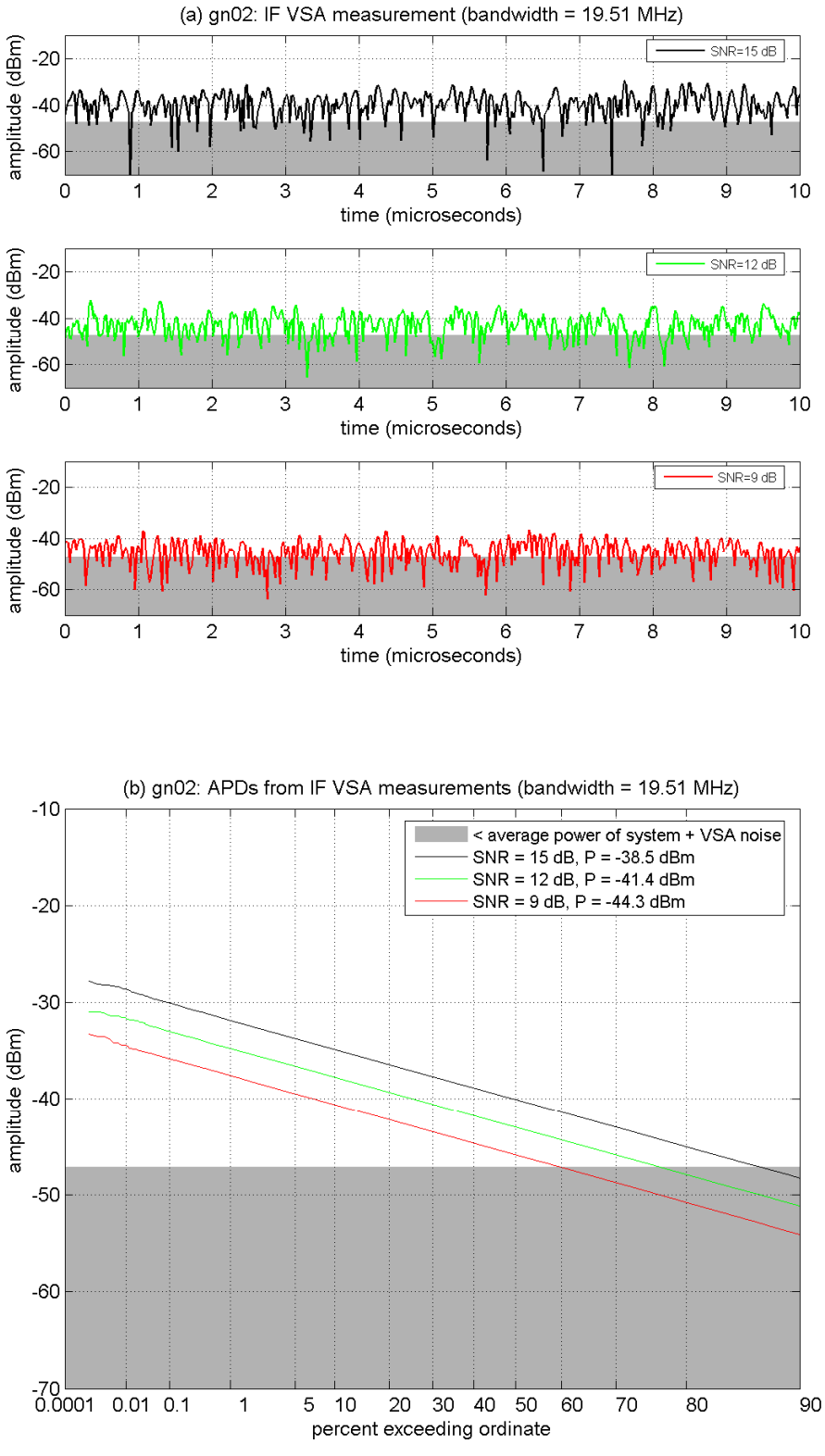

Figure D-6. IF measurements of GN-02 at INR_{TOV}.

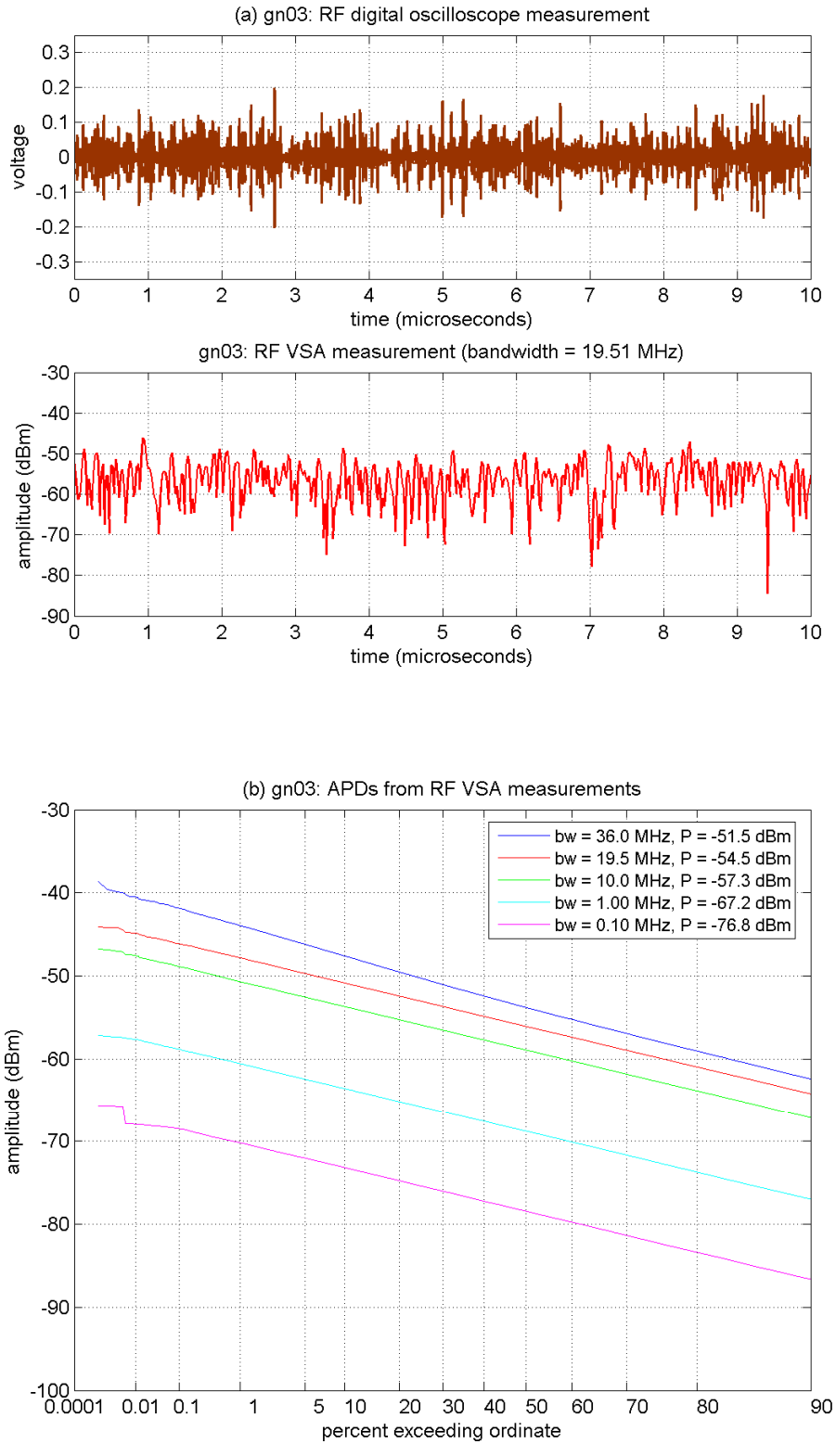

Figure D-7. RF measurements of GN-03 (τ_{on} = 10 ns, ζ = 0.2500).

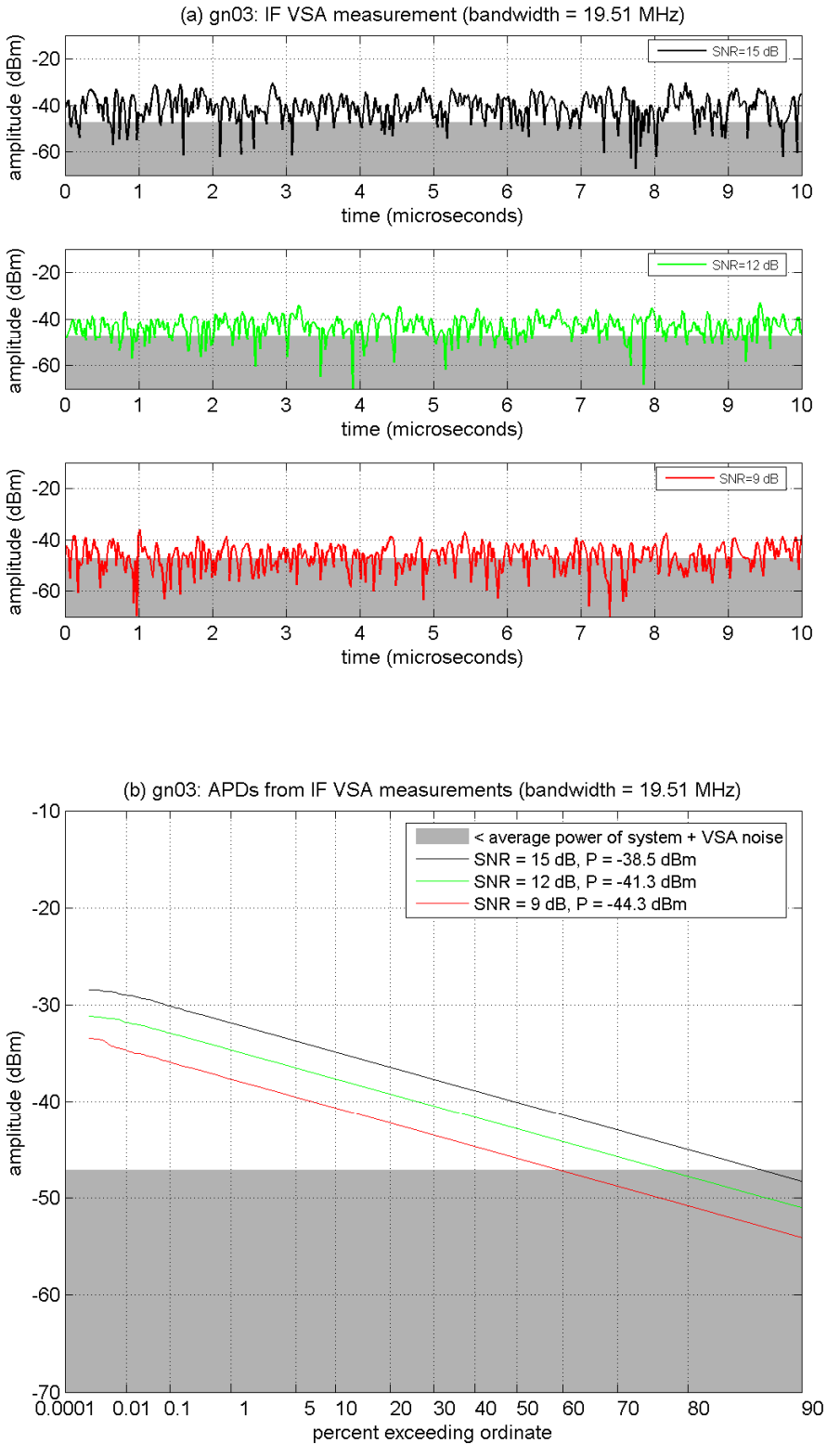

Figure D-8. IF measurements of GN-03 at INR_{TOV}.

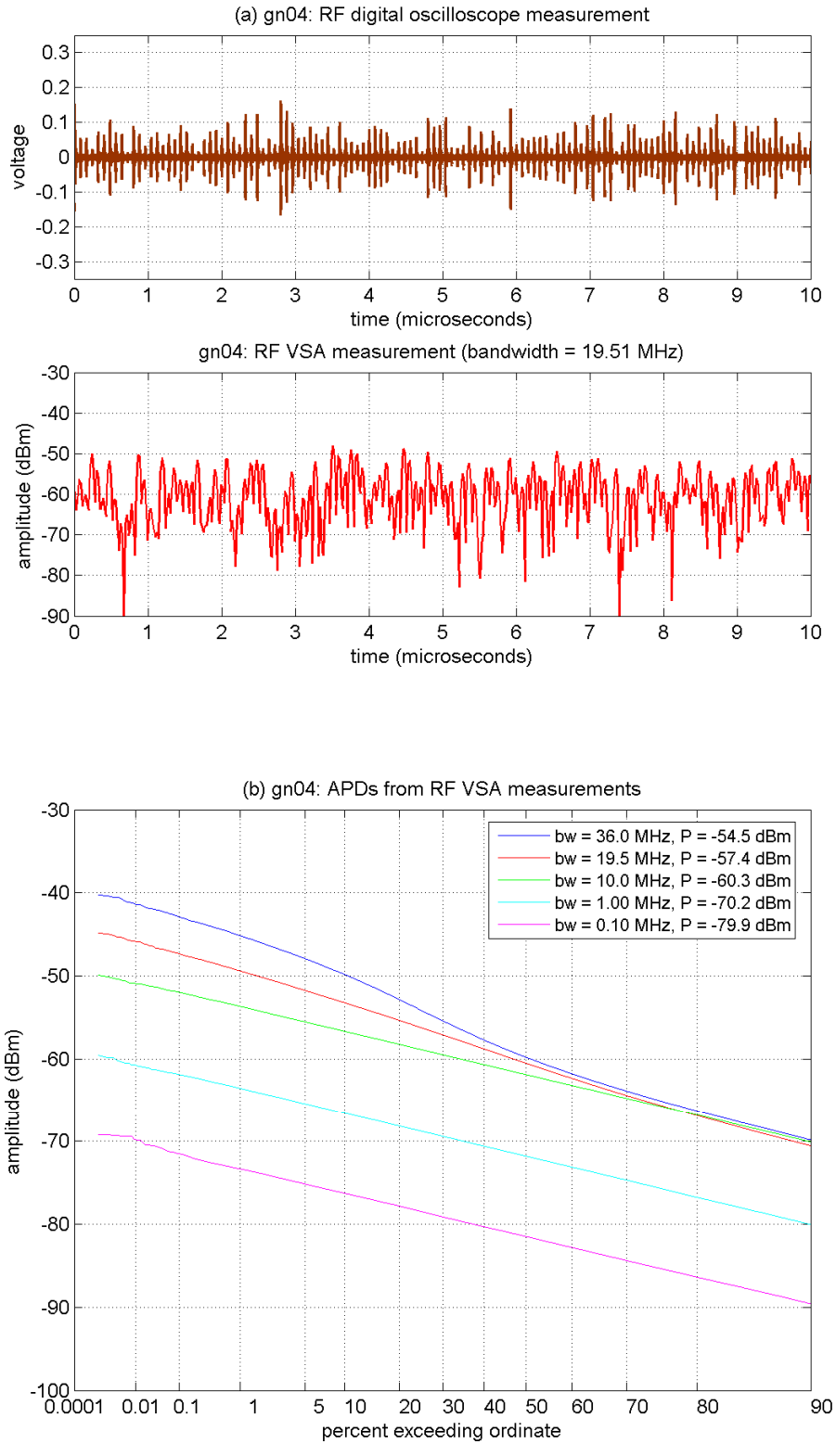

Figure D-9. RF measurements of GN-04 (τ_{on} = 10 ns, ζ = 0.1250).

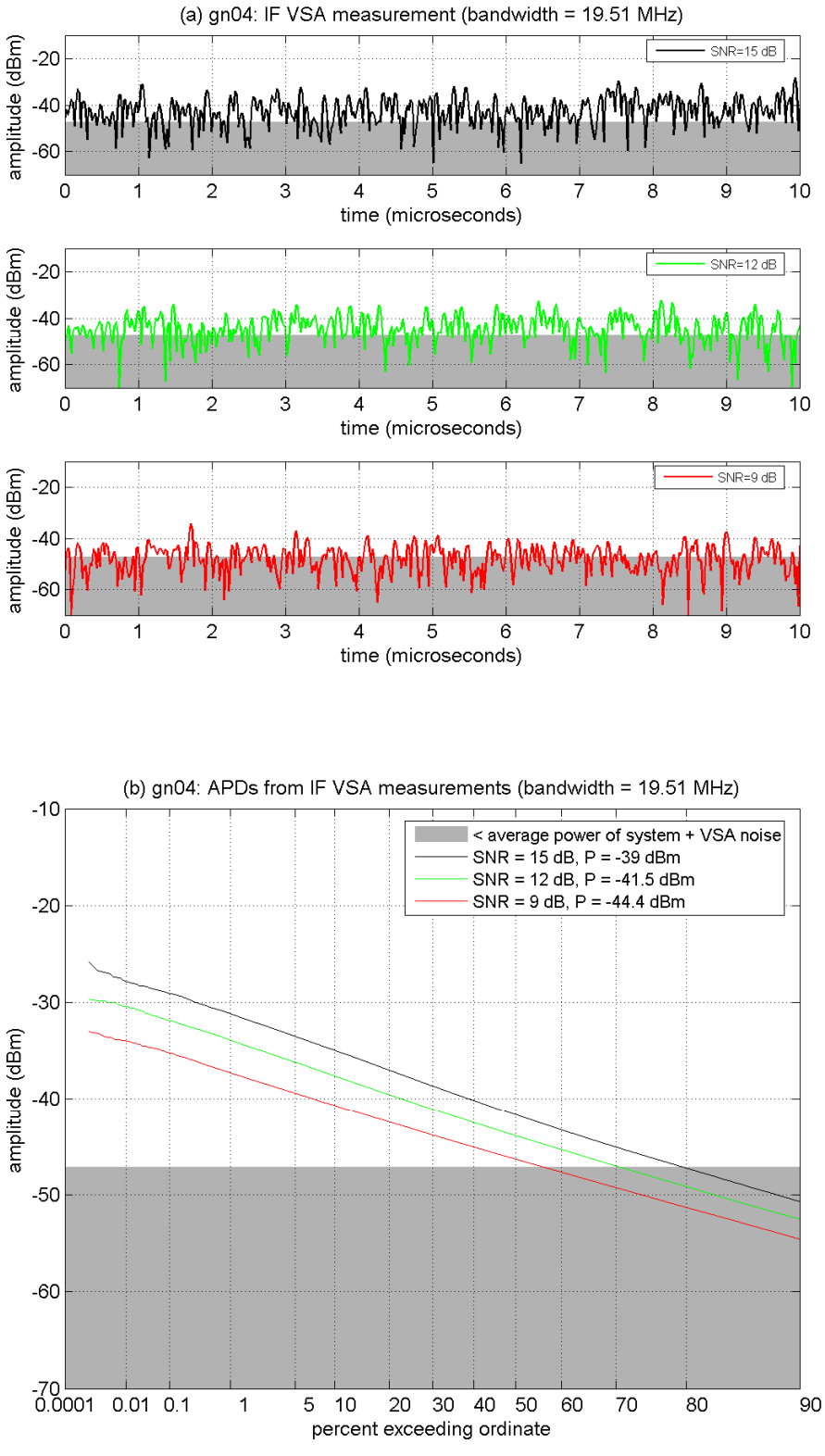

Figure D-10. IF measurements of GN-04 at INR_{TOV}.

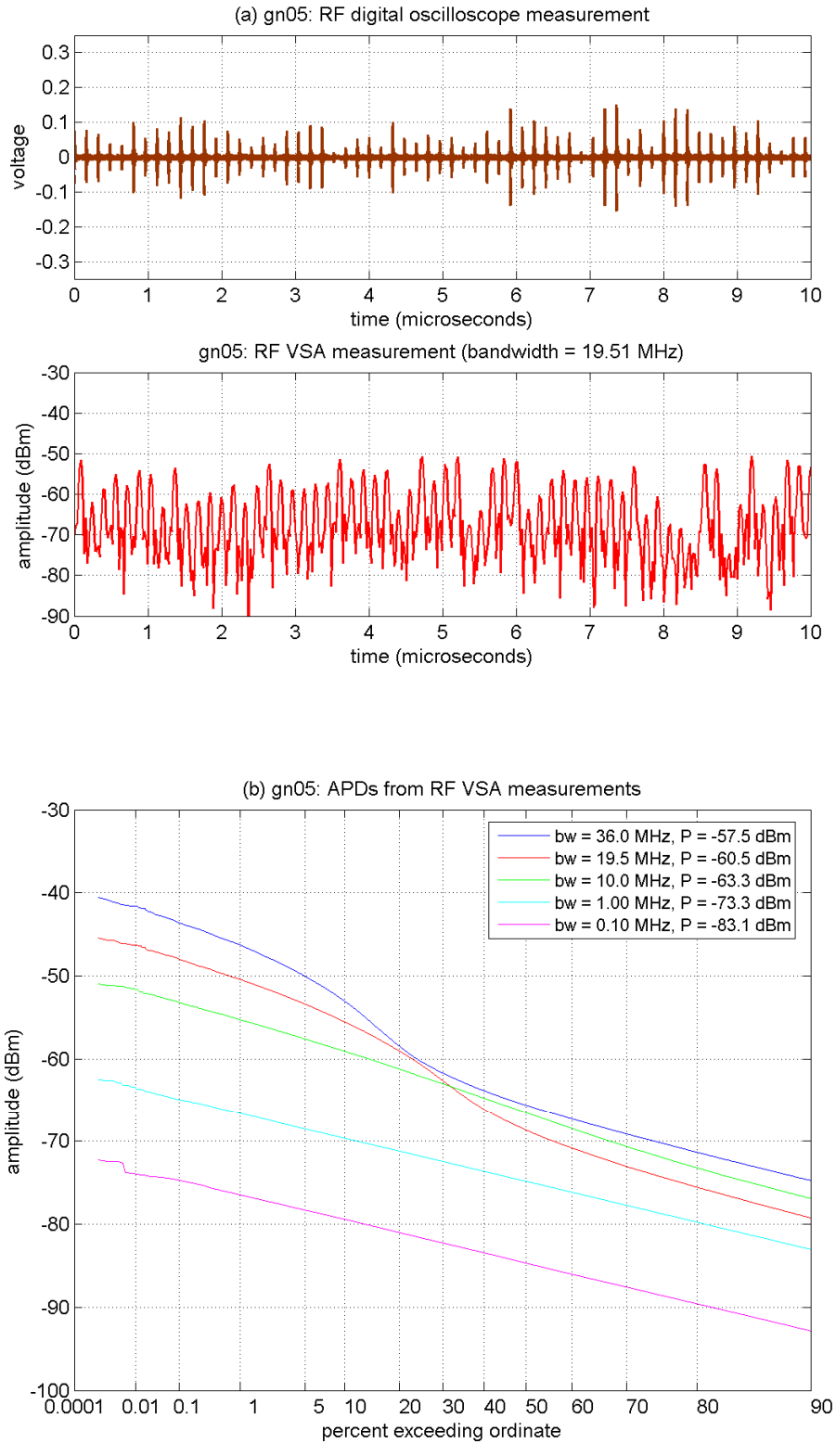

Figure D-11. RF measurements of GN-05 (τ_{on} = 10 ns, ζ = 0.0625).

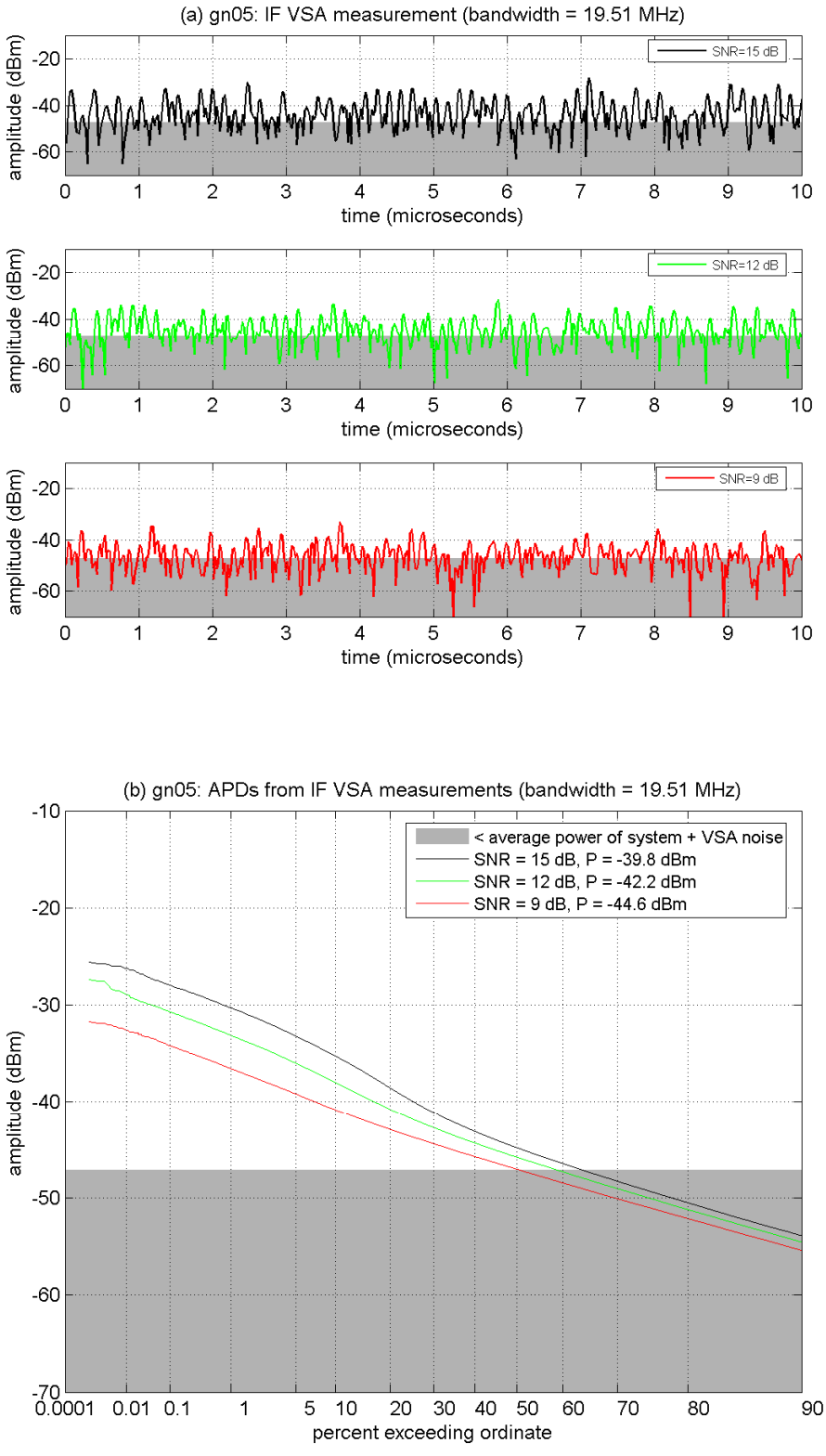

Figure D-12. IF measurements of GN-05 at INR_{TOV}.

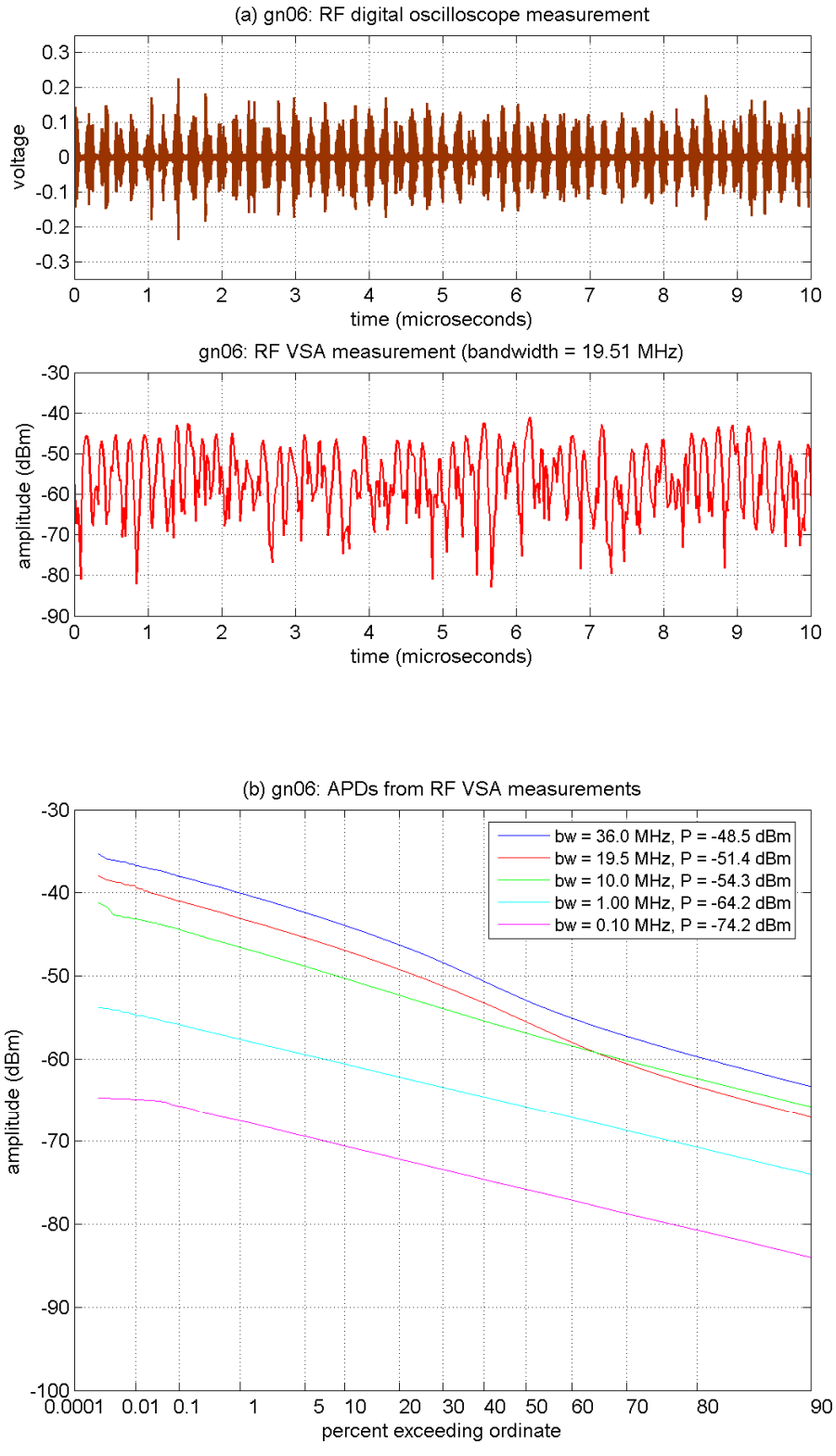

Figure D-13. RF measurements of GN-06 (τ_{on} = 100 ns, ζ = 0.5000).

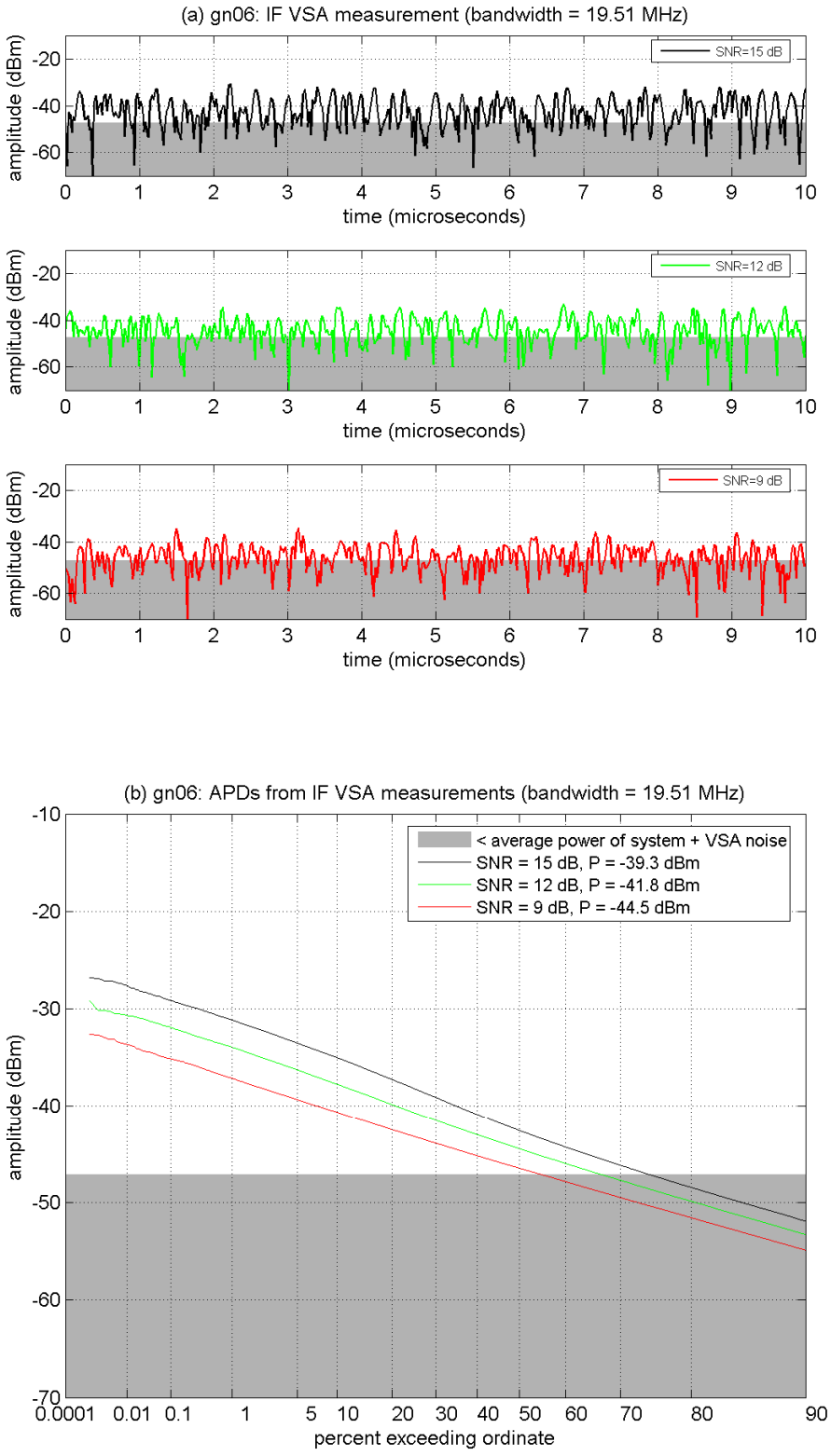

Figure D-14. IF measurements of GN-06 at INR_{TOV}.

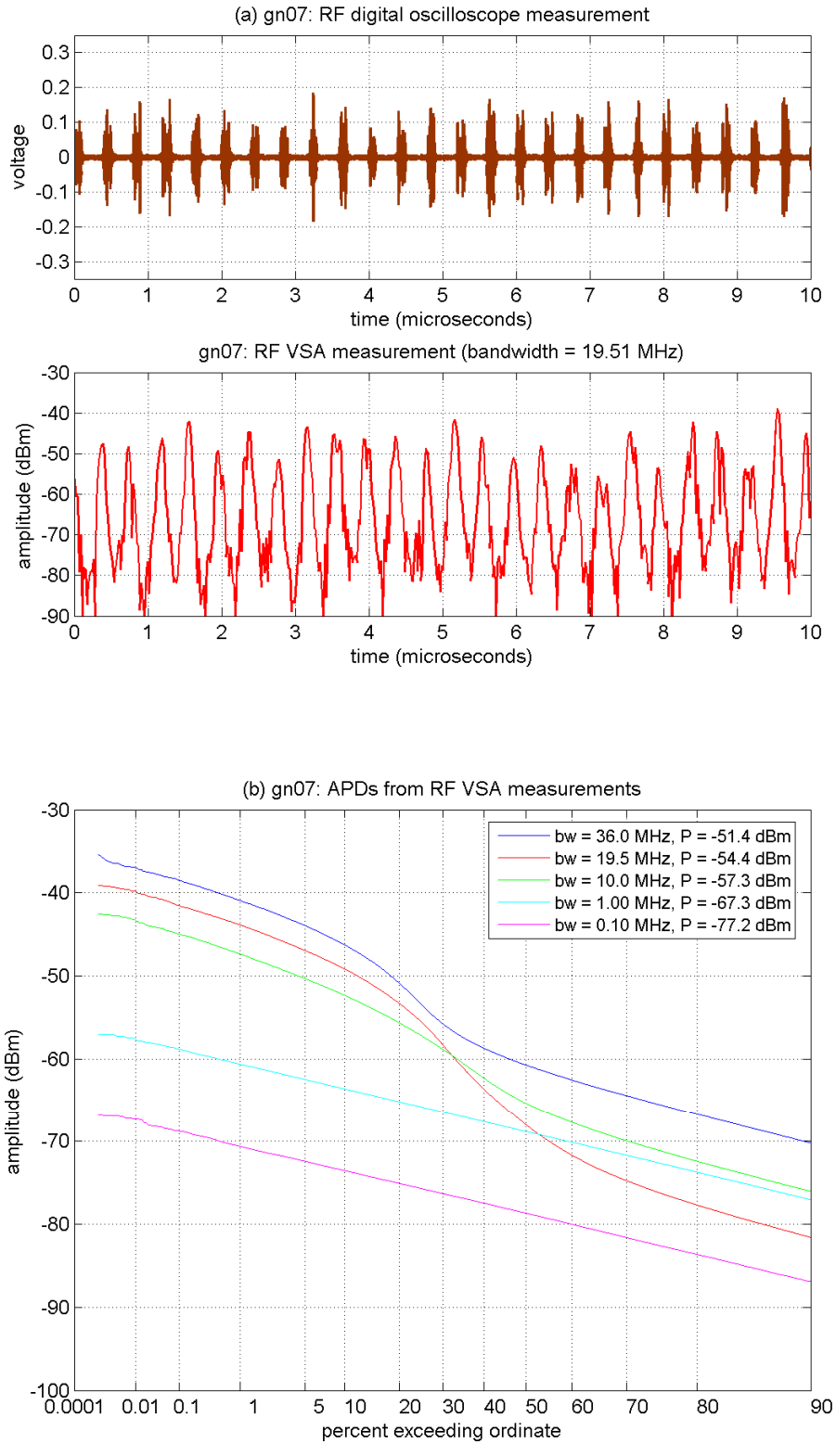

Figure D-15. RF measurements of GN-07 (τ_{on} = 100 ns, ζ = 0.2500).

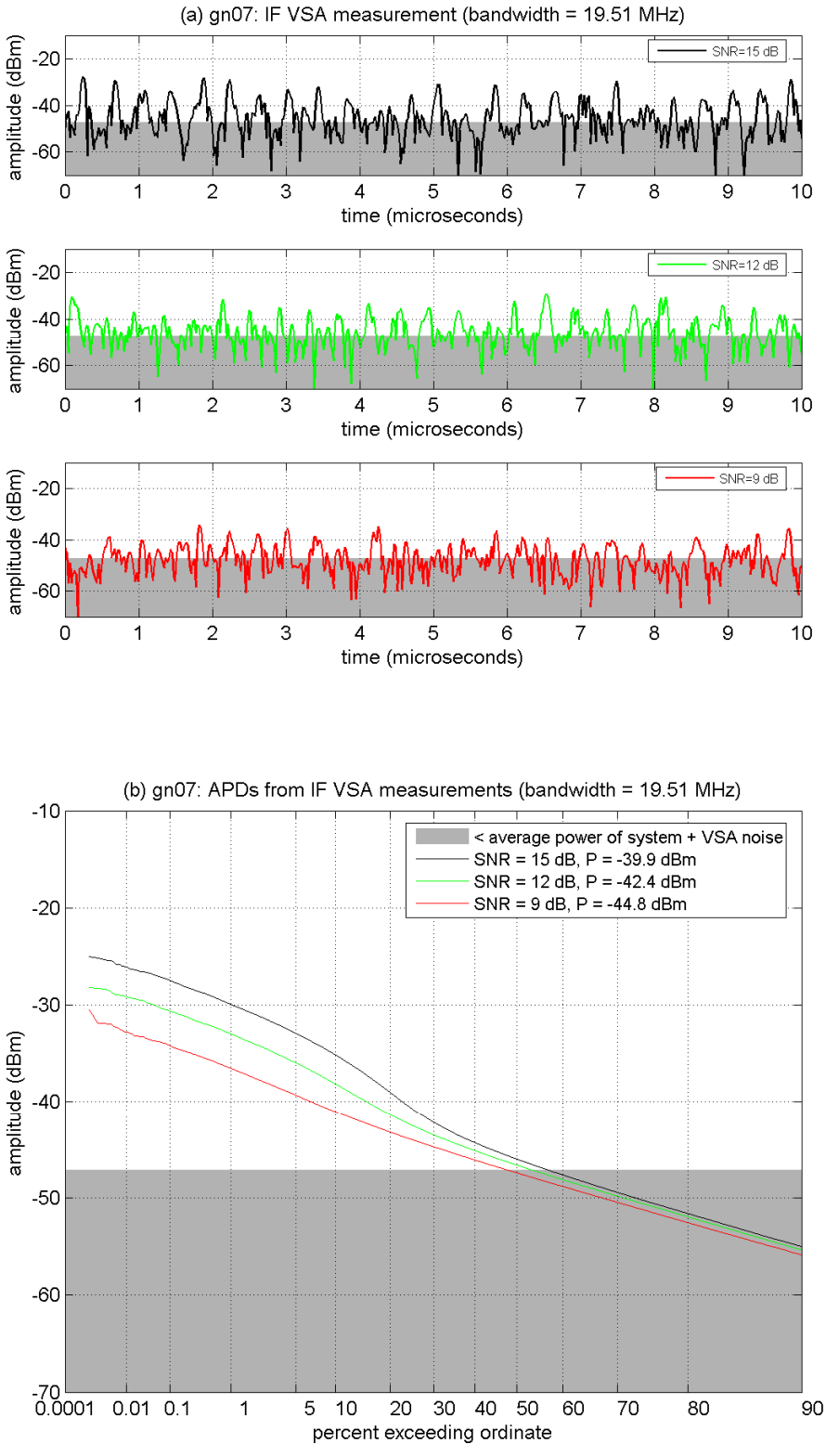

Figure D-16. IF measurements of GN-07 at INR_{TOV}.

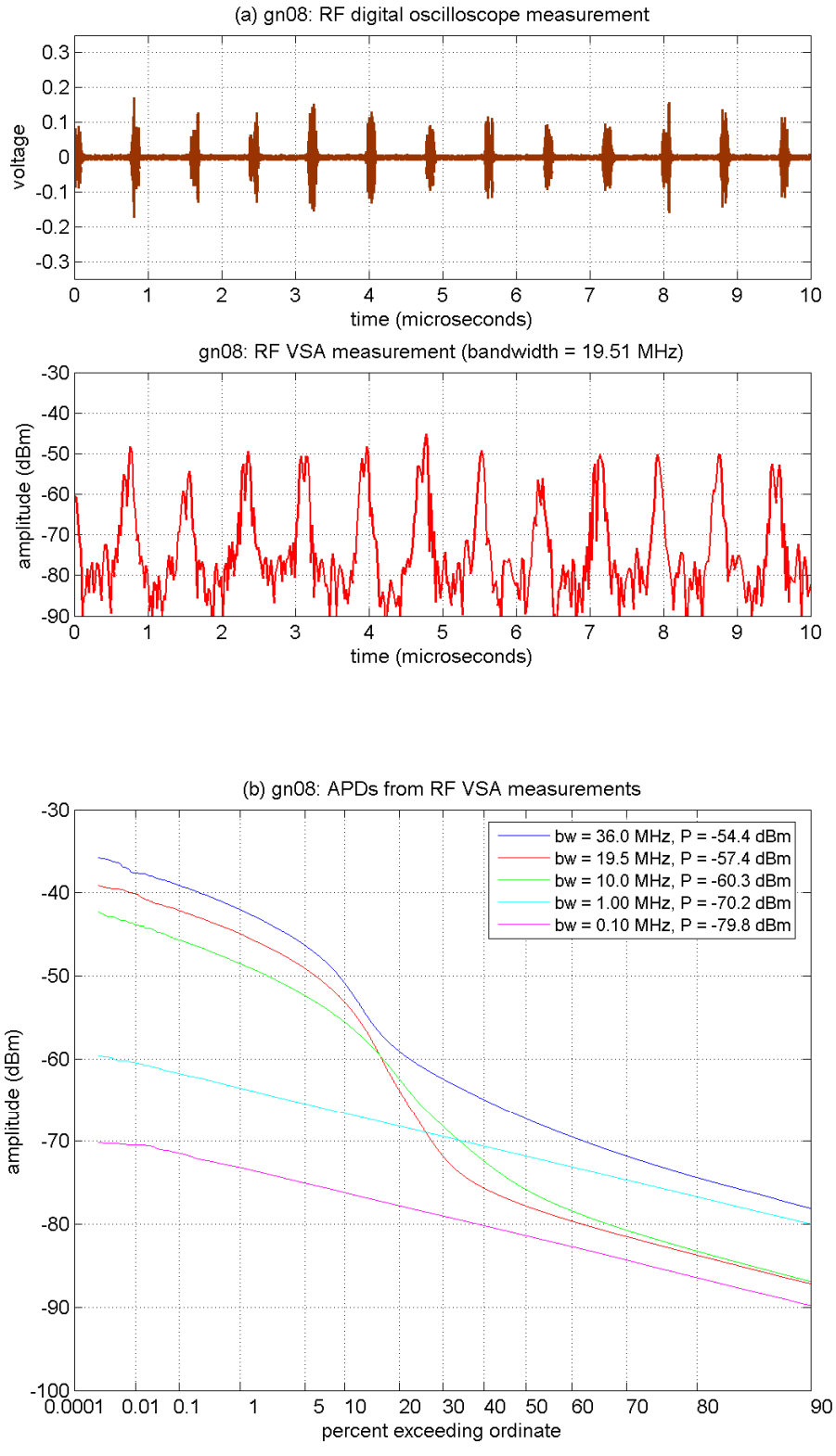

Figure D-17. RF measurements of GN-08 (τ_{on} = 100 ns, ζ = 0.1250).

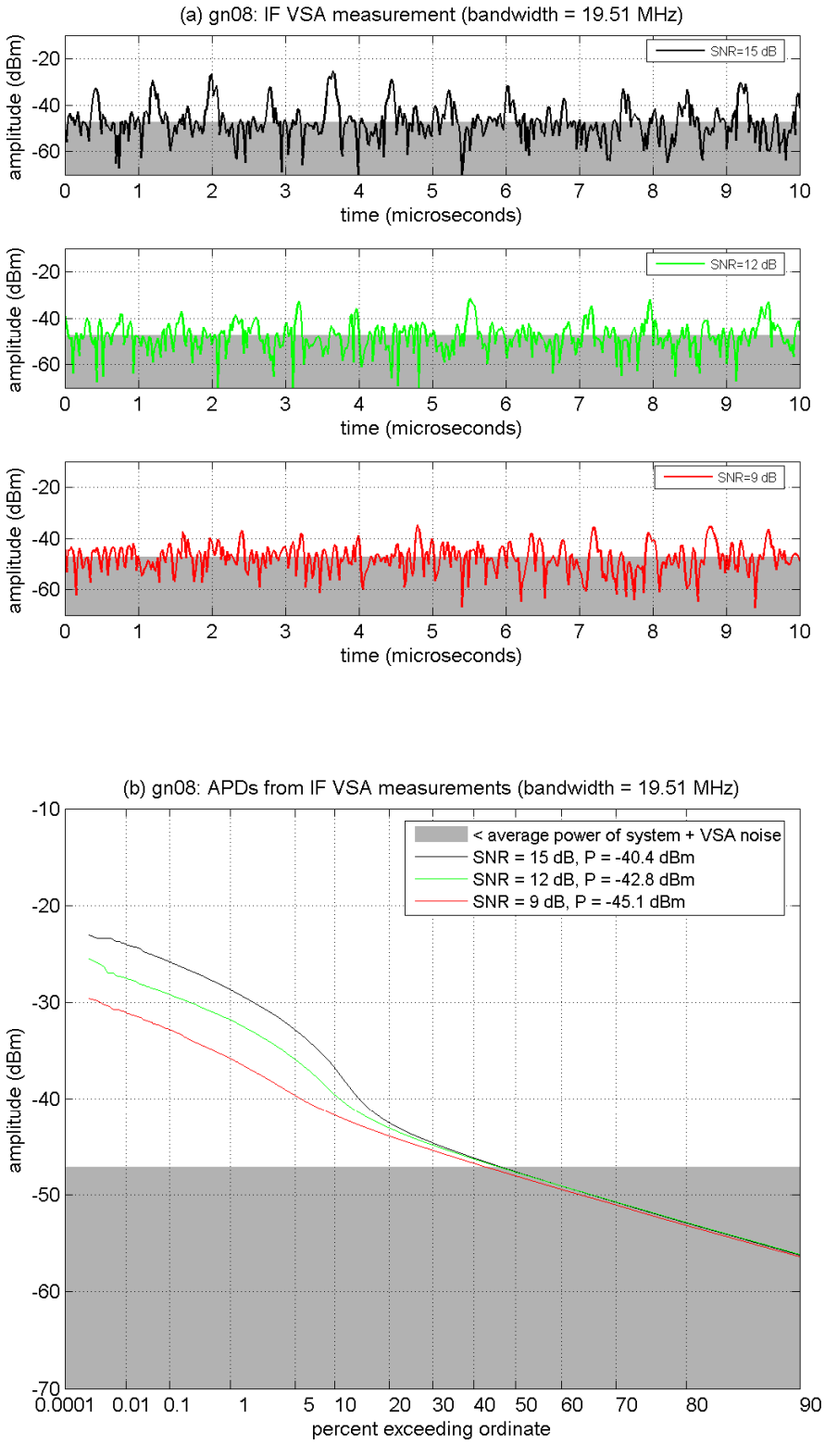

Figure D-18. IF measurements of GN-08 at INR_{TOV}.

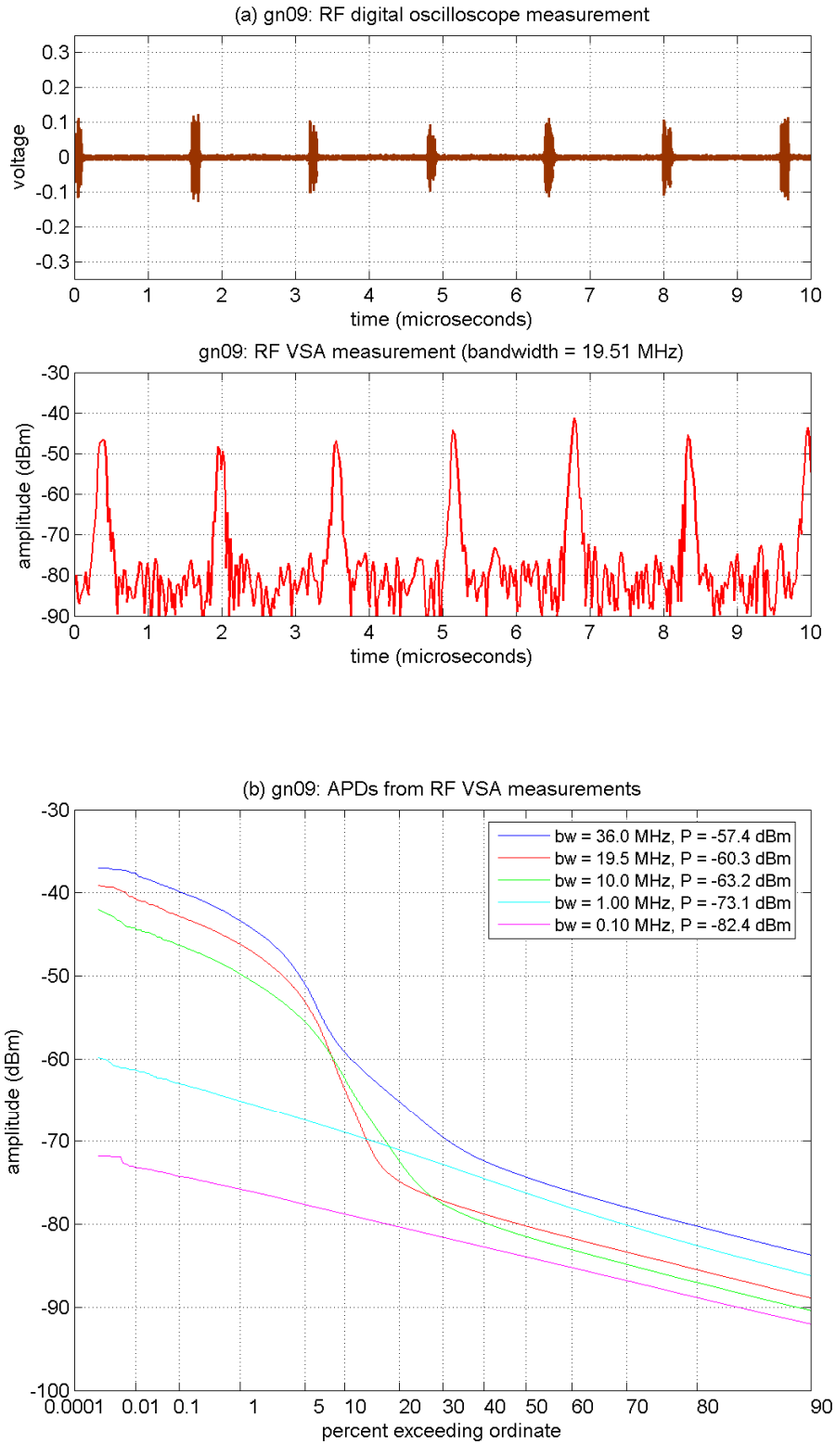

Figure D-19. RF measurements of GN-09 (τ_{on} = 100 ns, ζ = 0.0625).

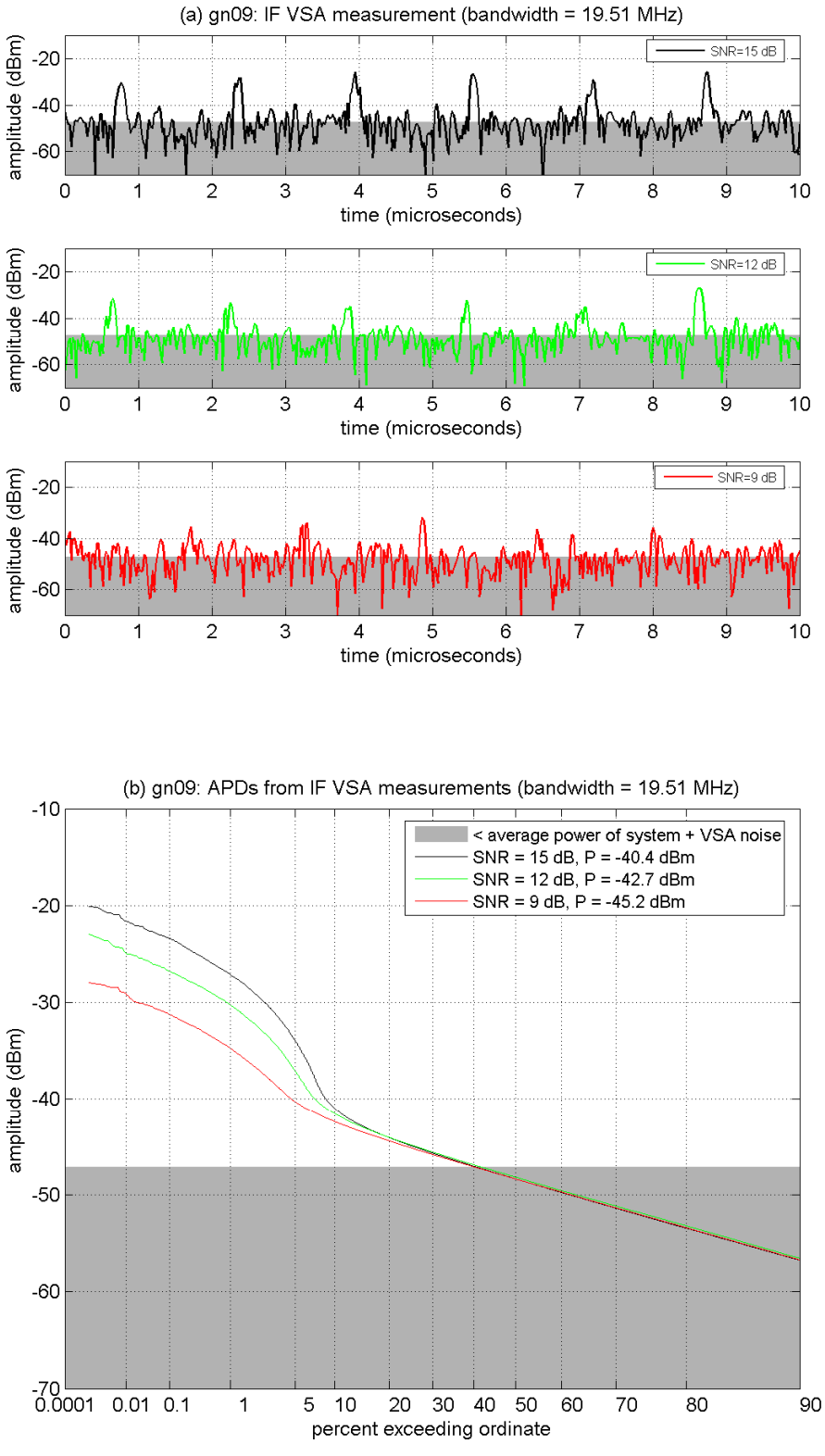

Figure D-20. IF measurements of GN-09 at INR_{TOV}.

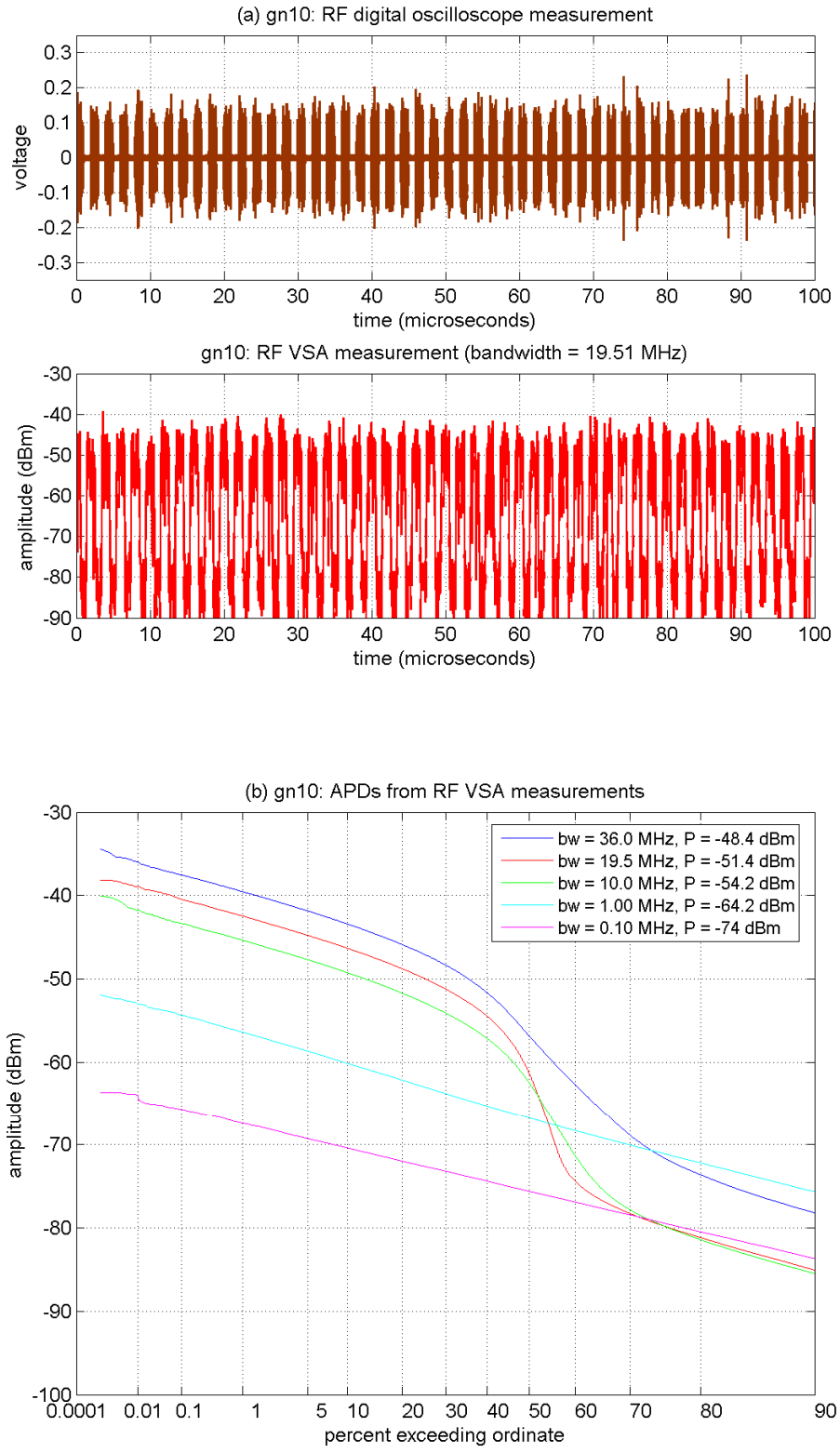

Figure D-21. RF measurements of GN-10 (τ_{on} = 1000 ns, ζ = 0.5000).

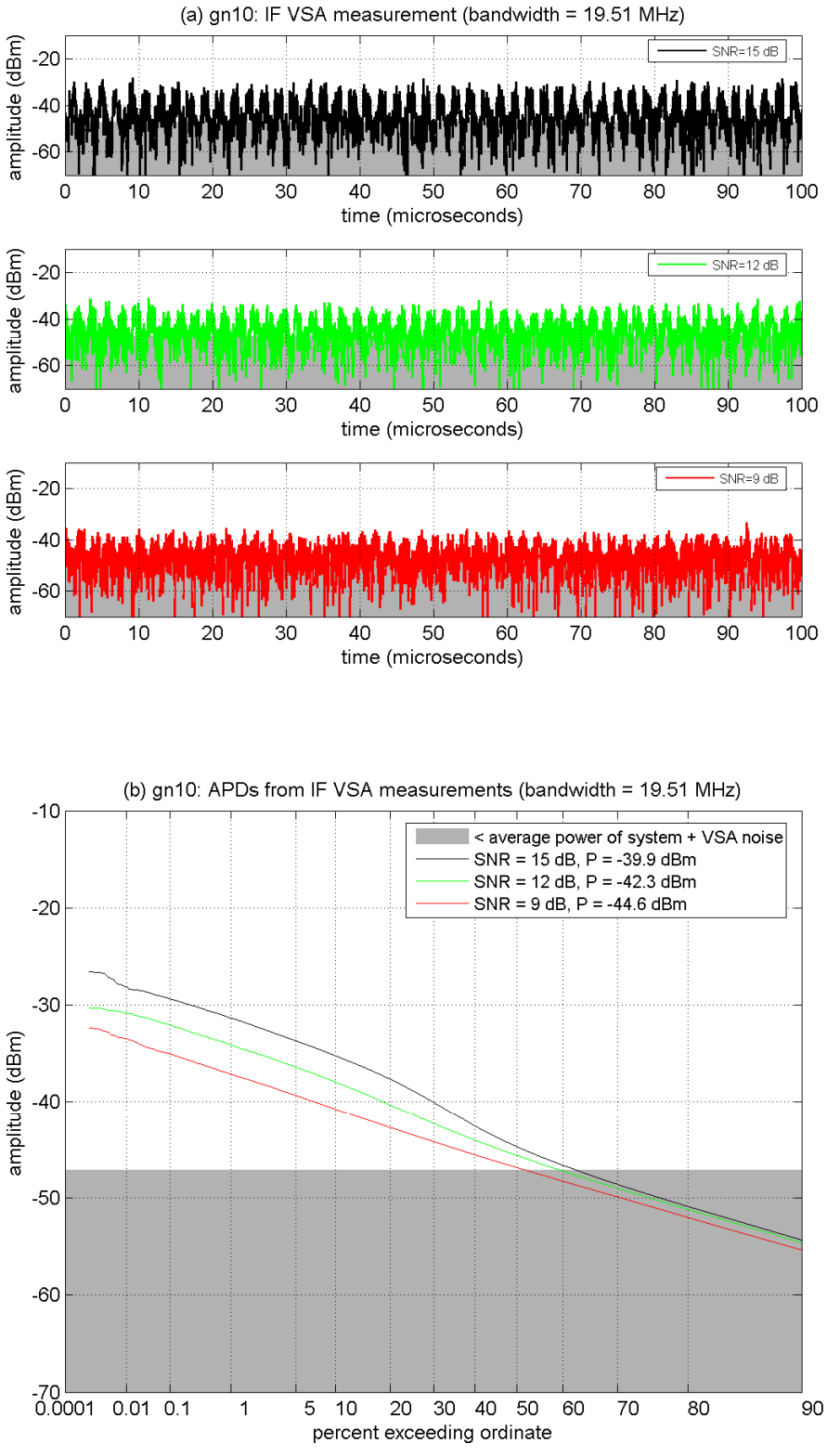

Figure D-22. IF measurements of GN-10 at INR_{TOV}.

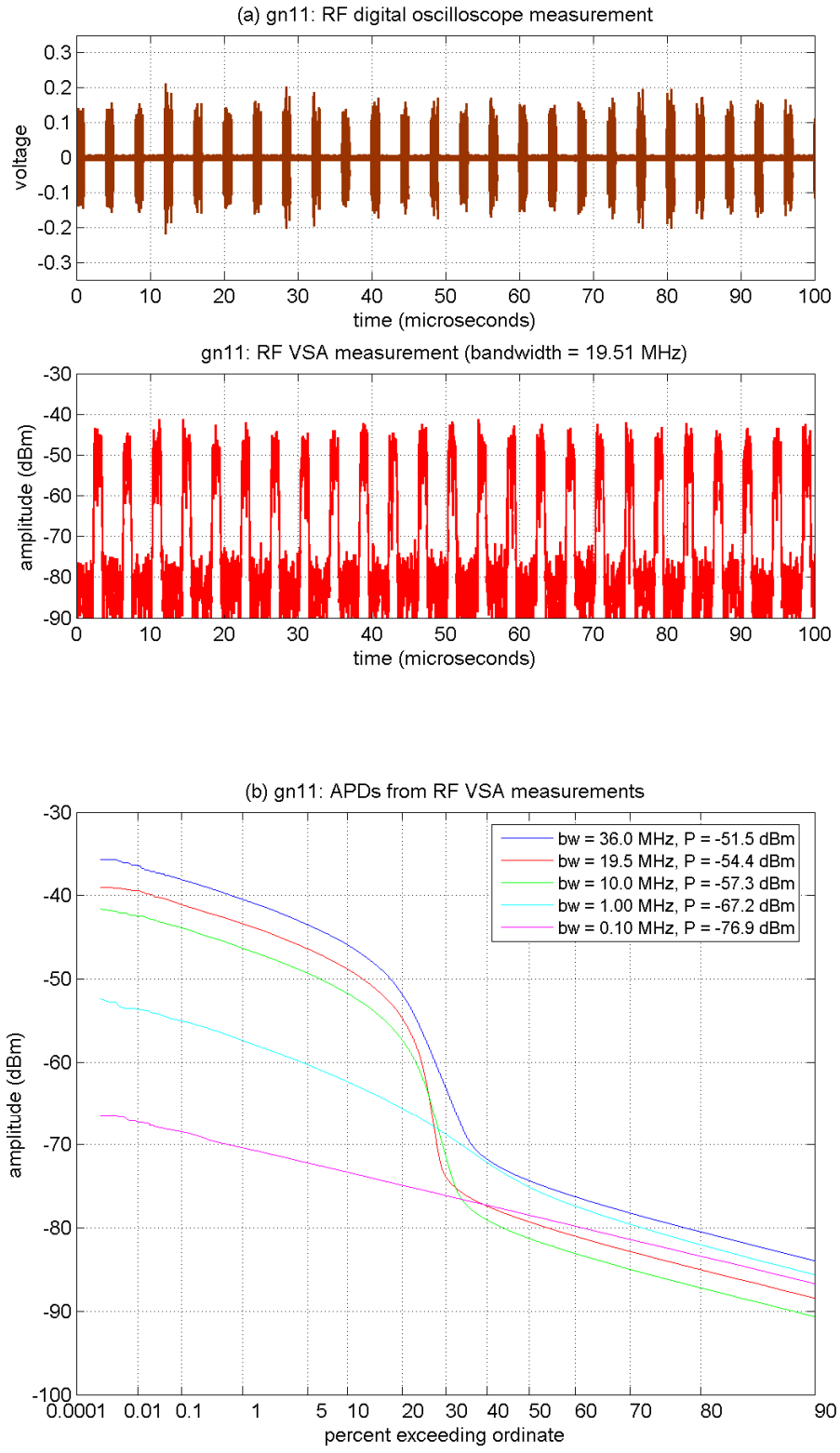

Figure D-23. RF measurements of GN-11 (τ_{on} = 1000 ns, ζ = 0.2500).

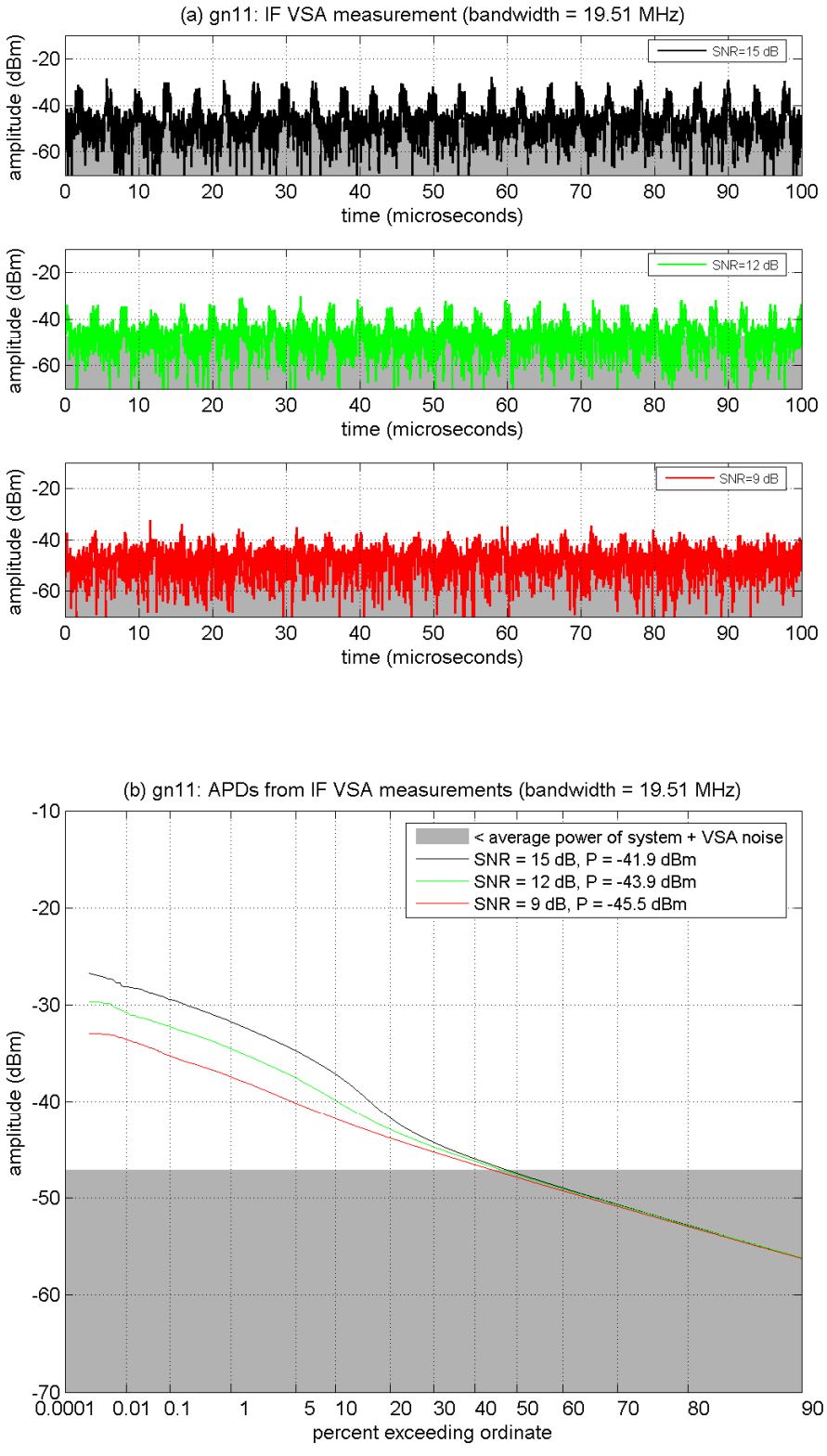

Figure D-24. IF measurements of GN-11 at INR_{TOV}.

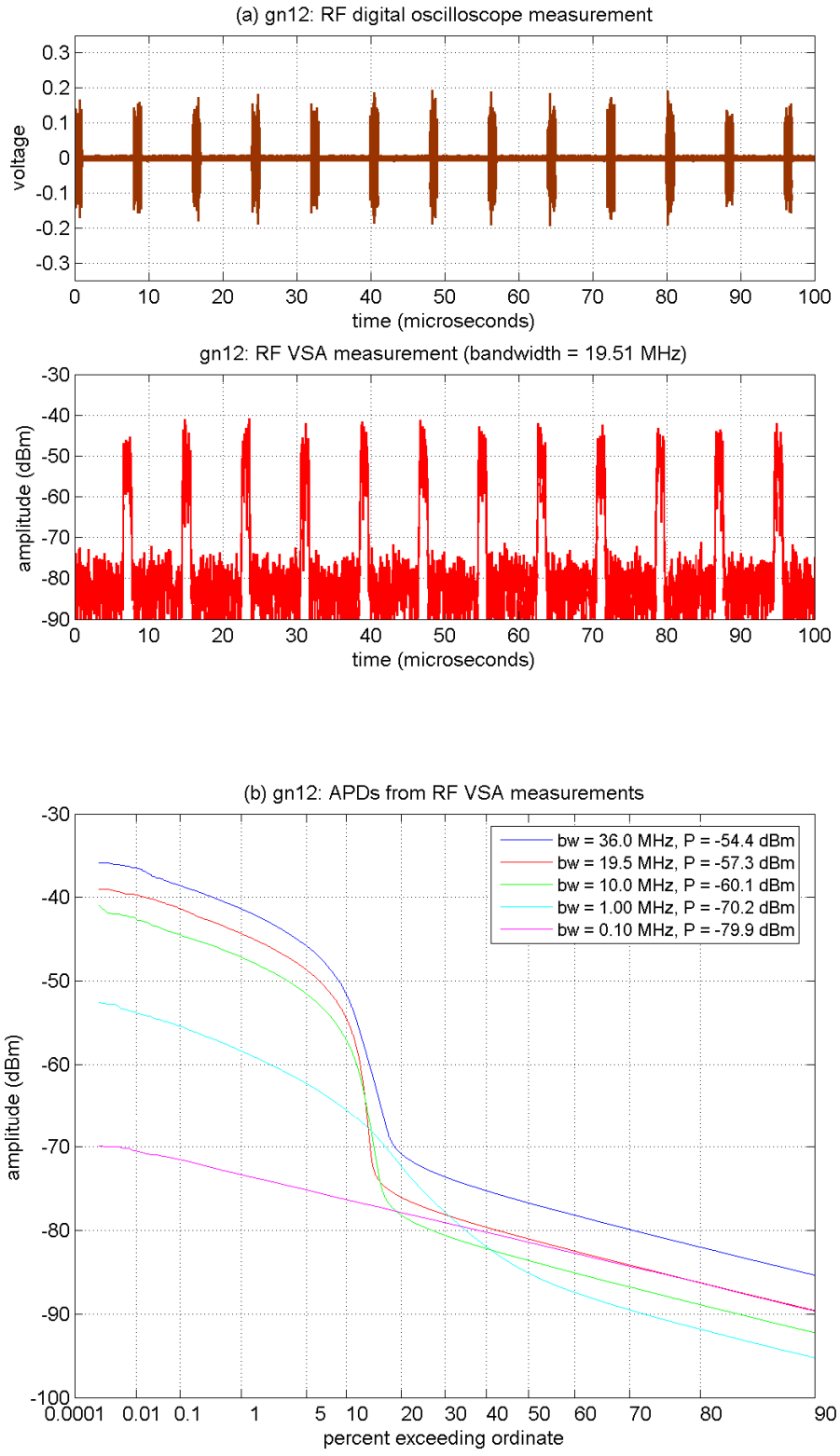

Figure D-25. RF measurements of GN-12 (τ_{on} = 1000 ns, ζ = 0.1250).

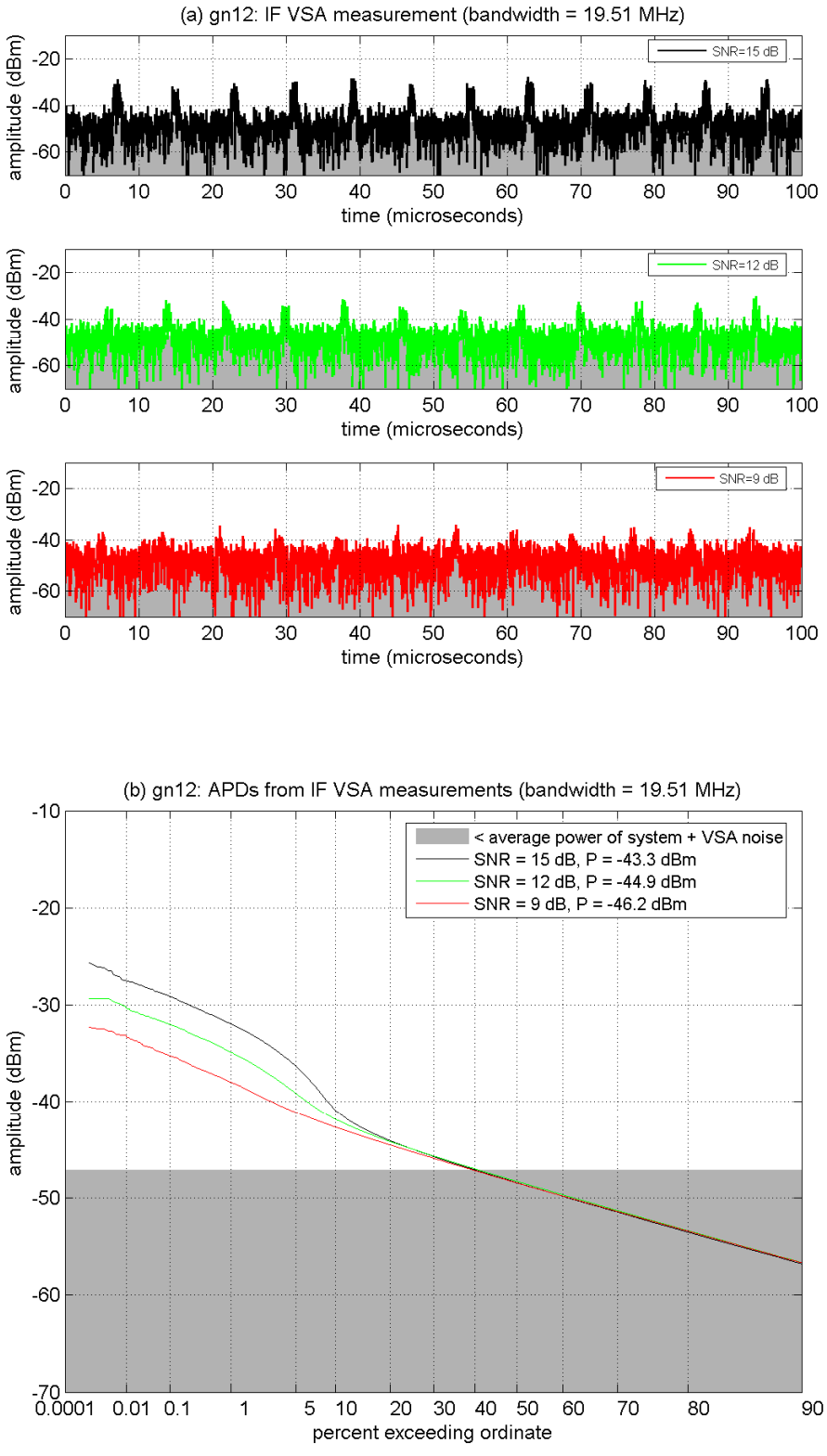

Figure D-26. IF measurements of GN-12 at INR_{TOV}.

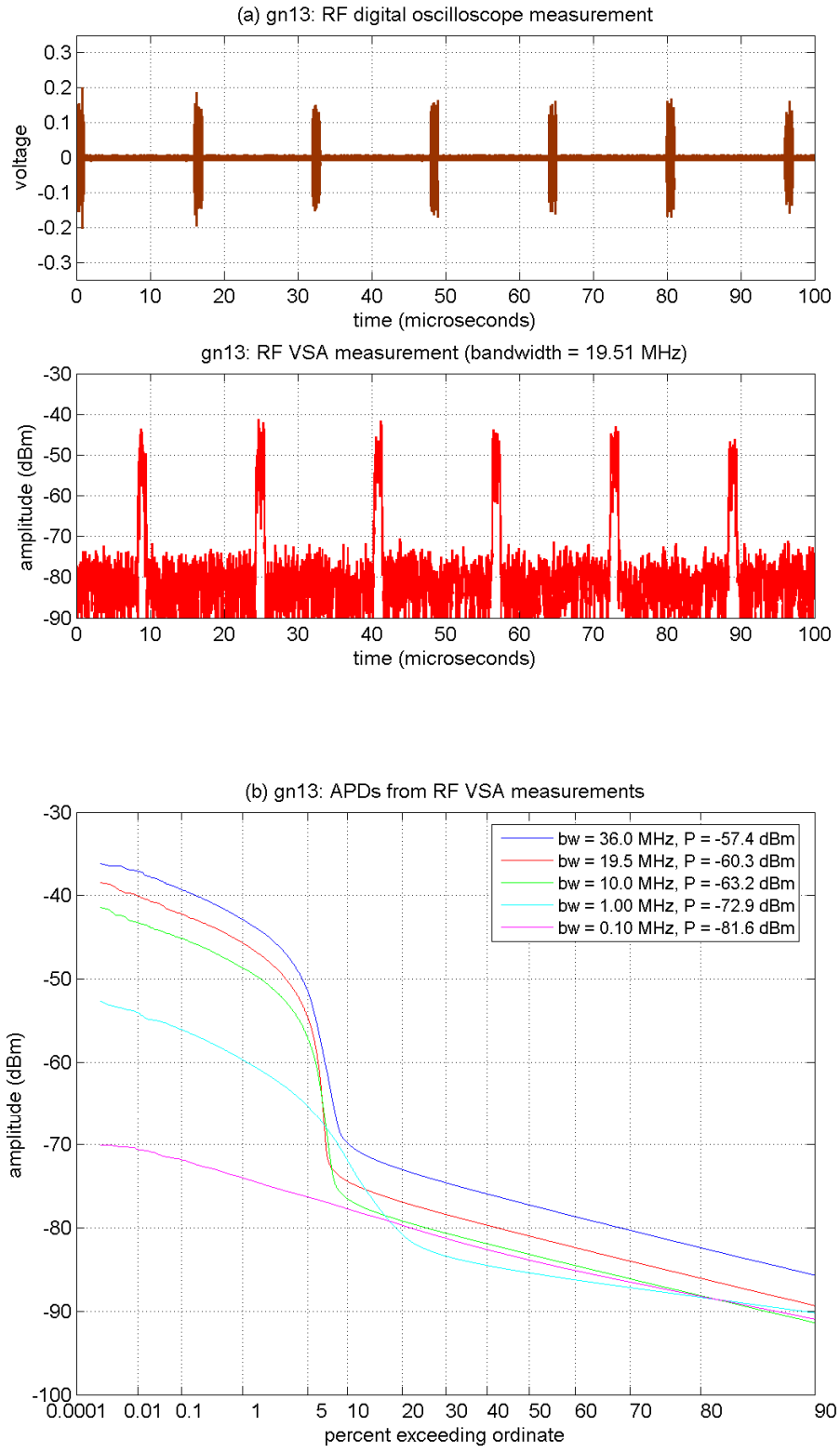

Figure D-27. RF measurements of GN-13 (τ_{on} = 1000 ns, ζ = 0.0625).

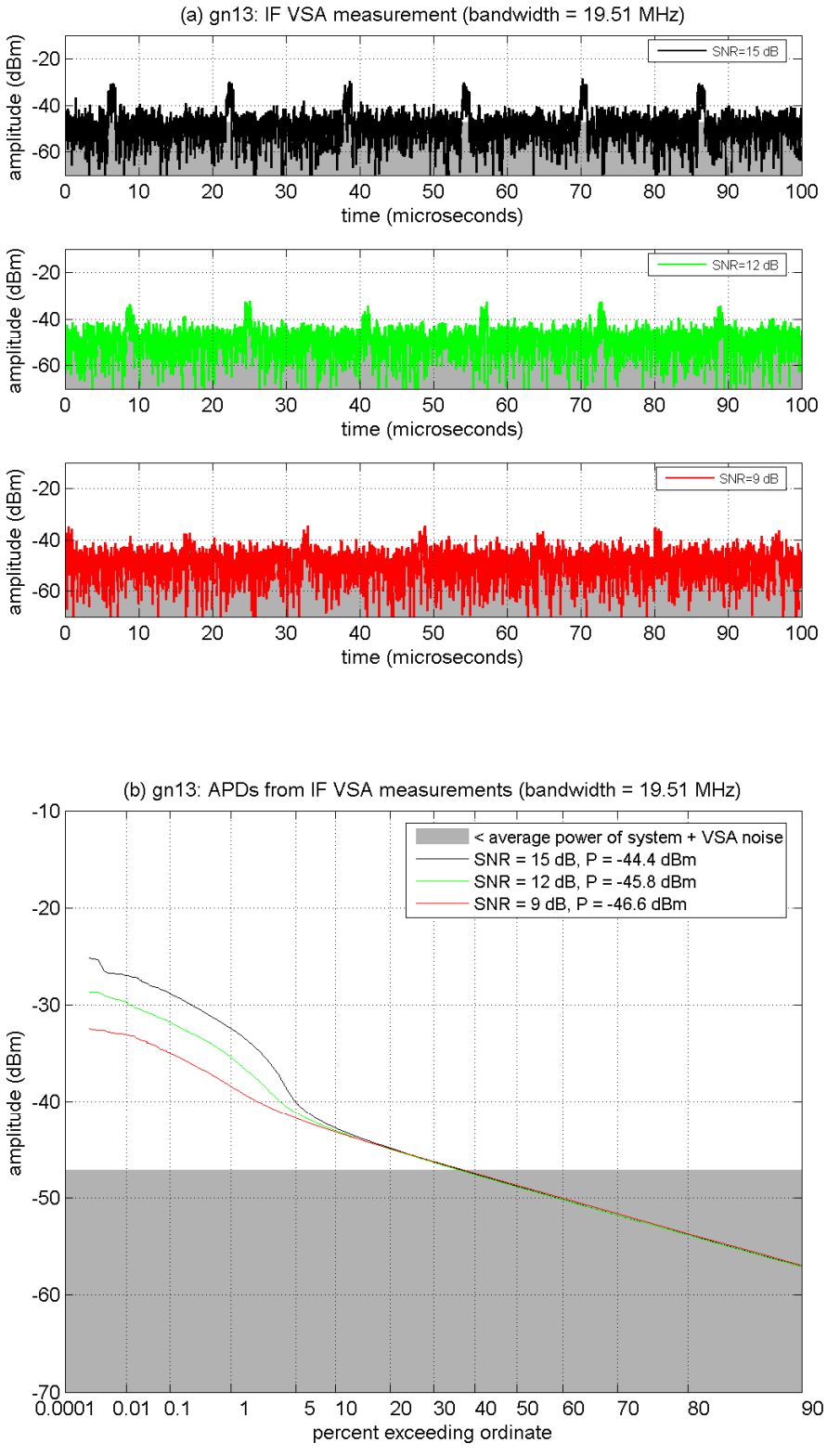

Figure D-28. IF measurements of GN-13 at INR_{TOV}.

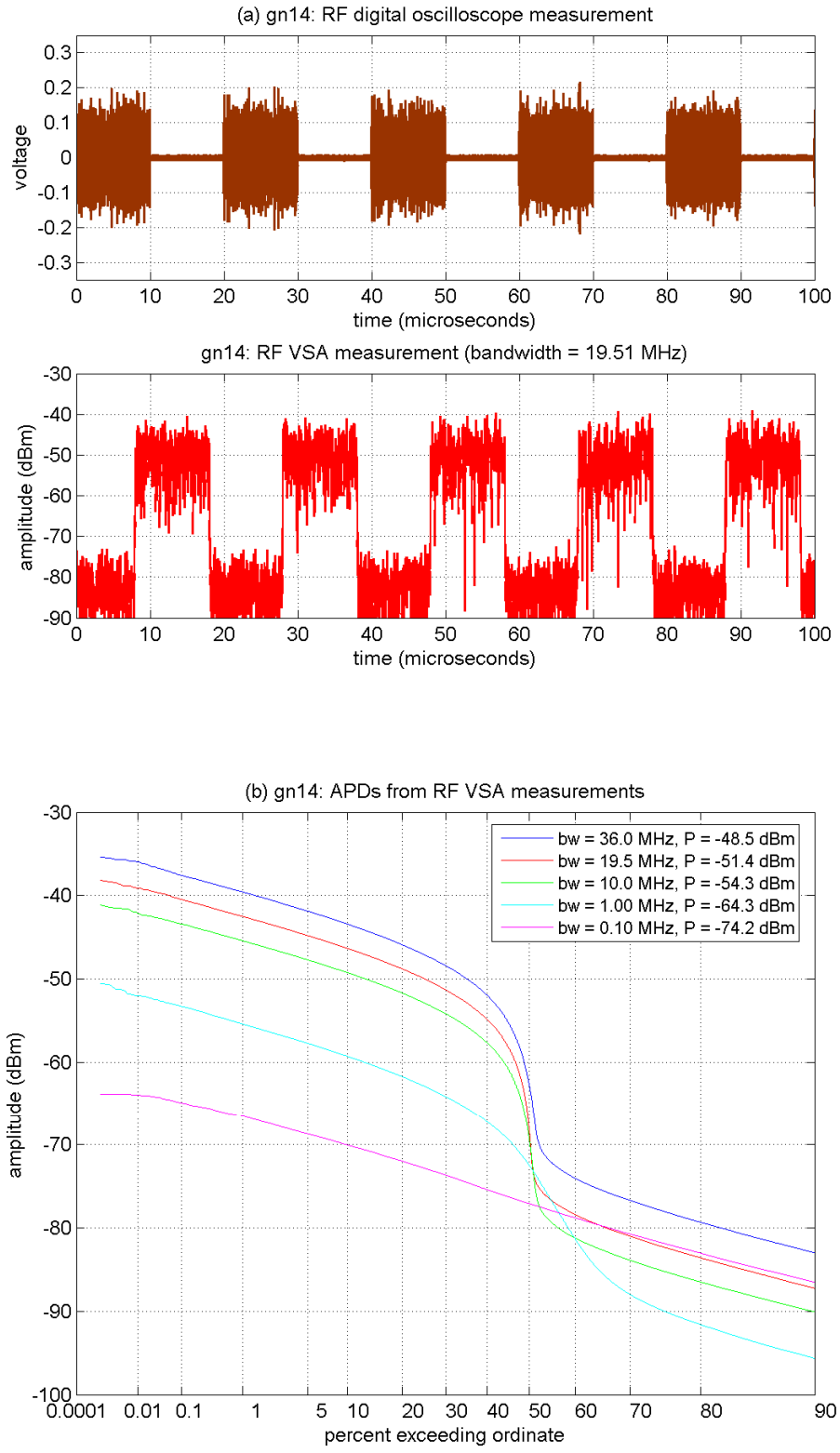

Figure D-29. RF measurements of GN-14 (τ_{on} = 10000 ns, ζ = 0.5000).

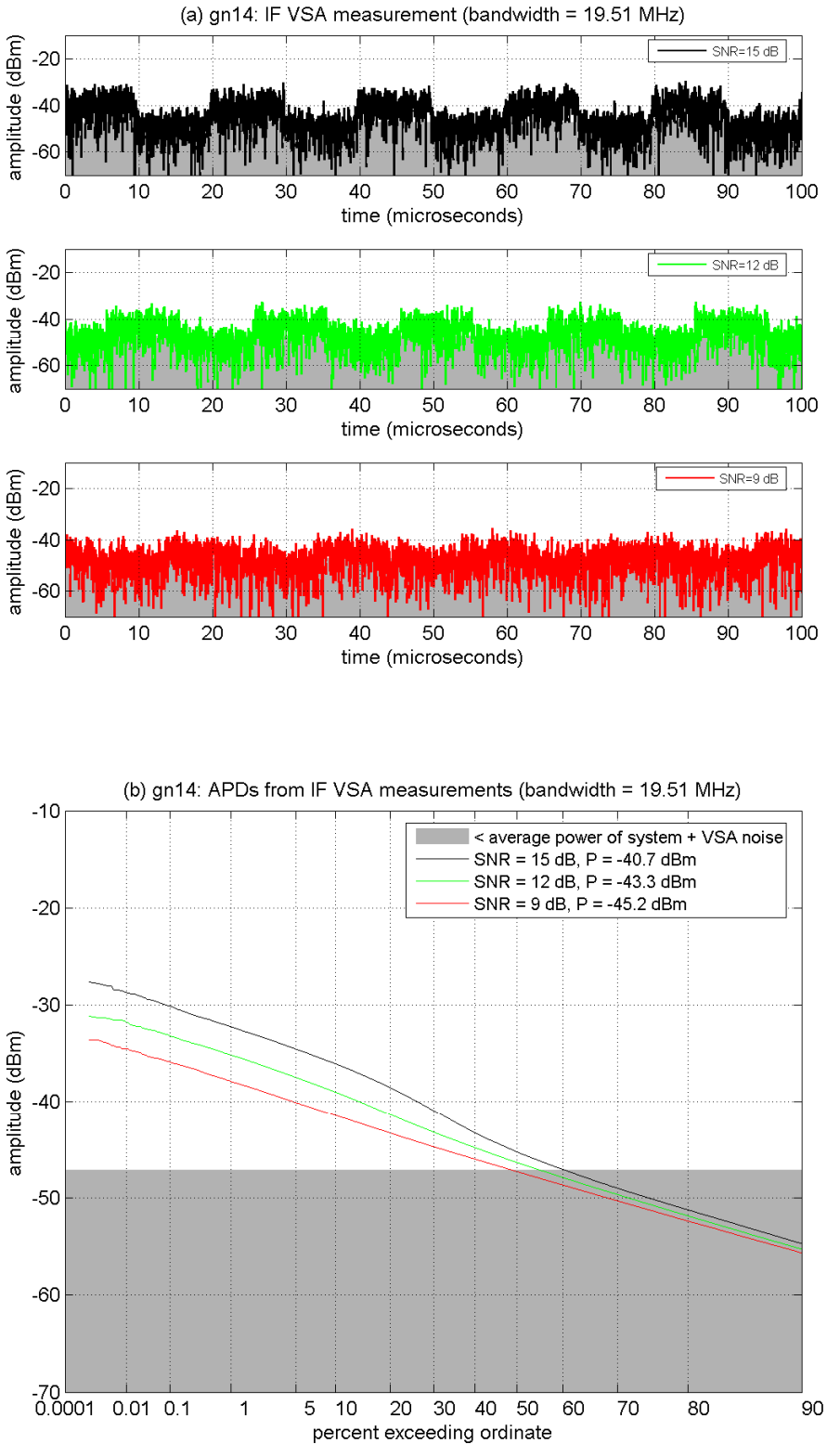

Figure D-30. IF measurements of GN-14 at INR_{TOV}.

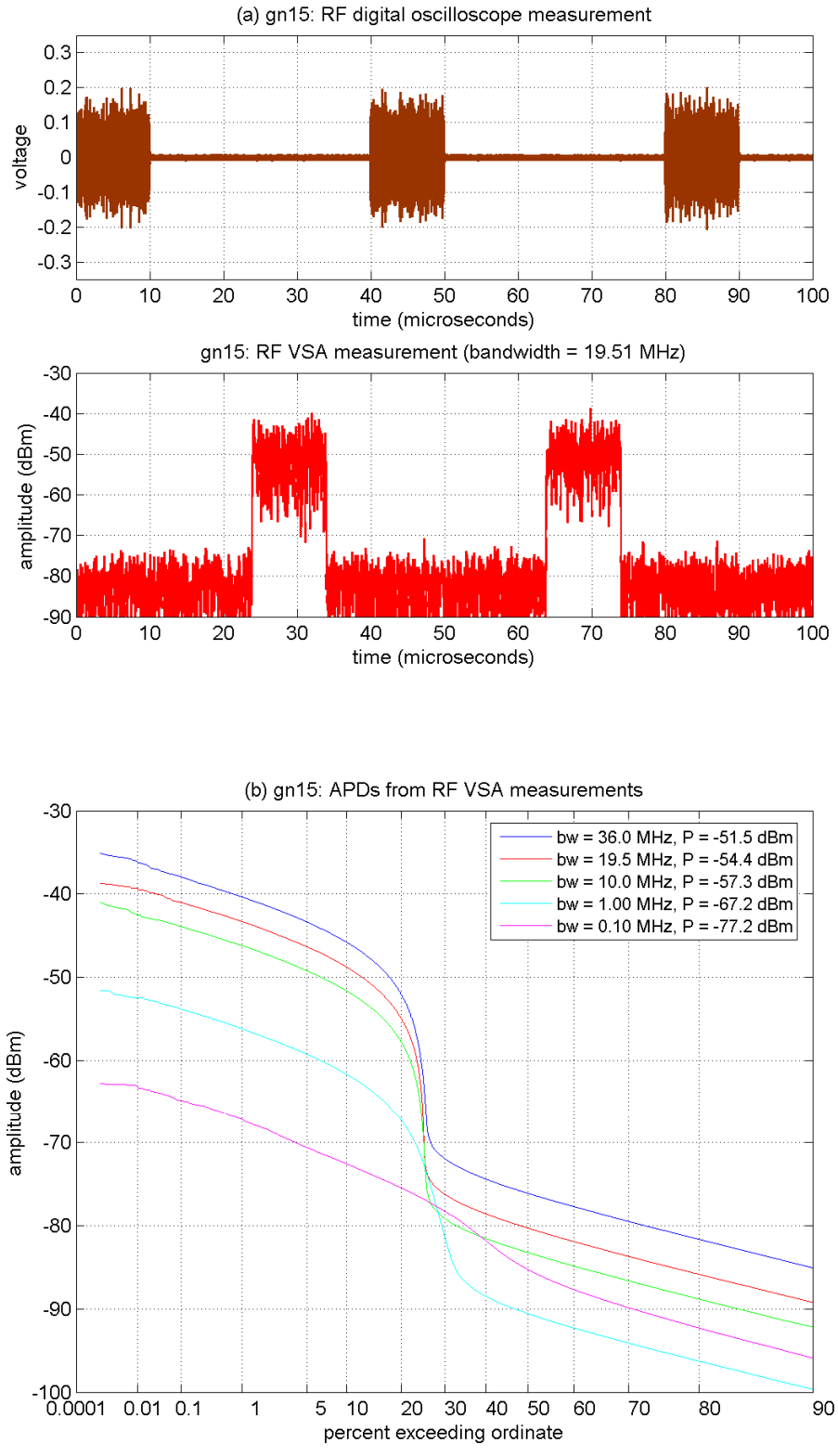

Figure D-31. RF measurements of GN-15 (τ_{on} = 10000 ns, ζ = 0.2500).

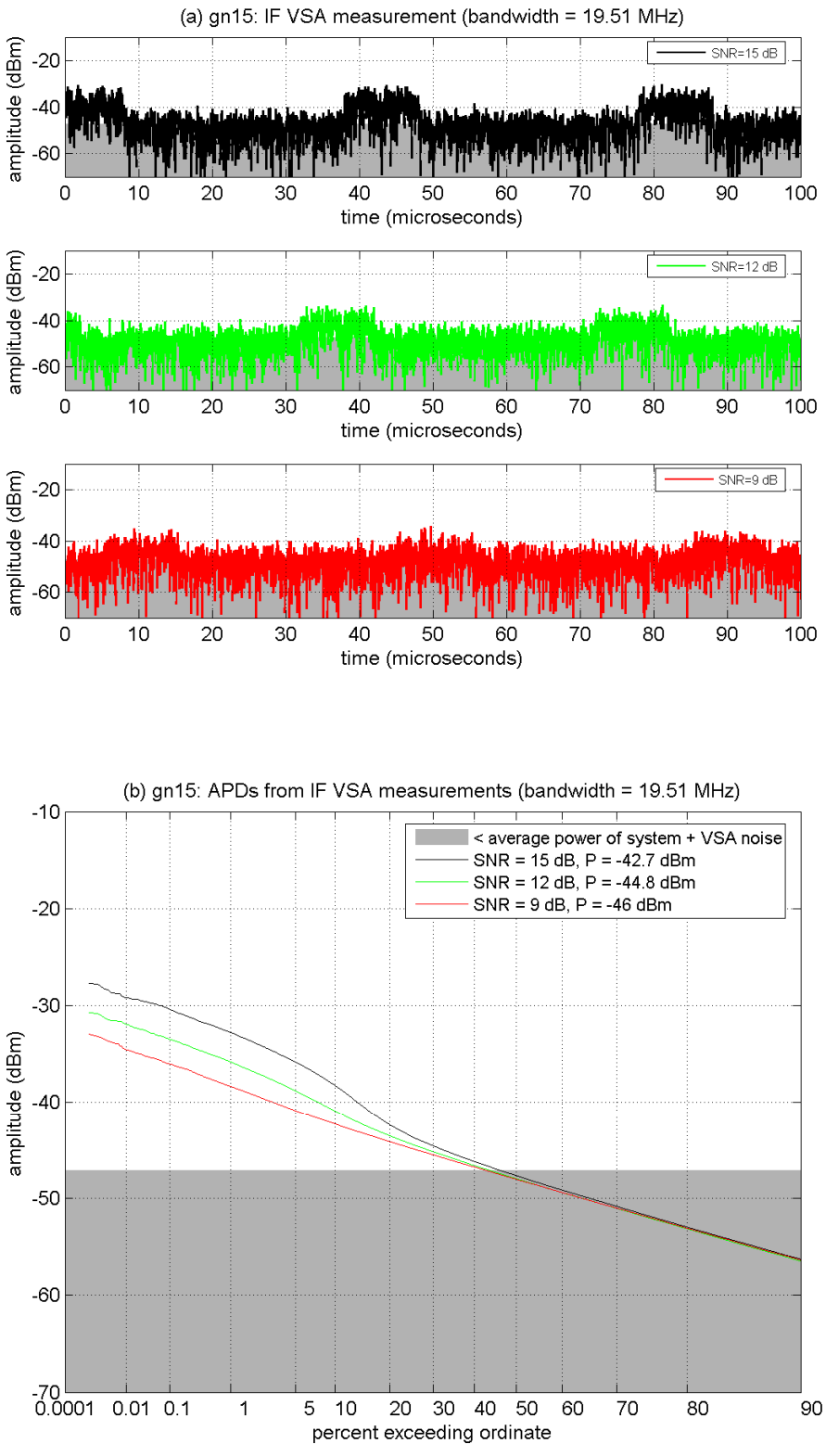

Figure D-32. IF measurements of GN-15 at INR_{TOV}.

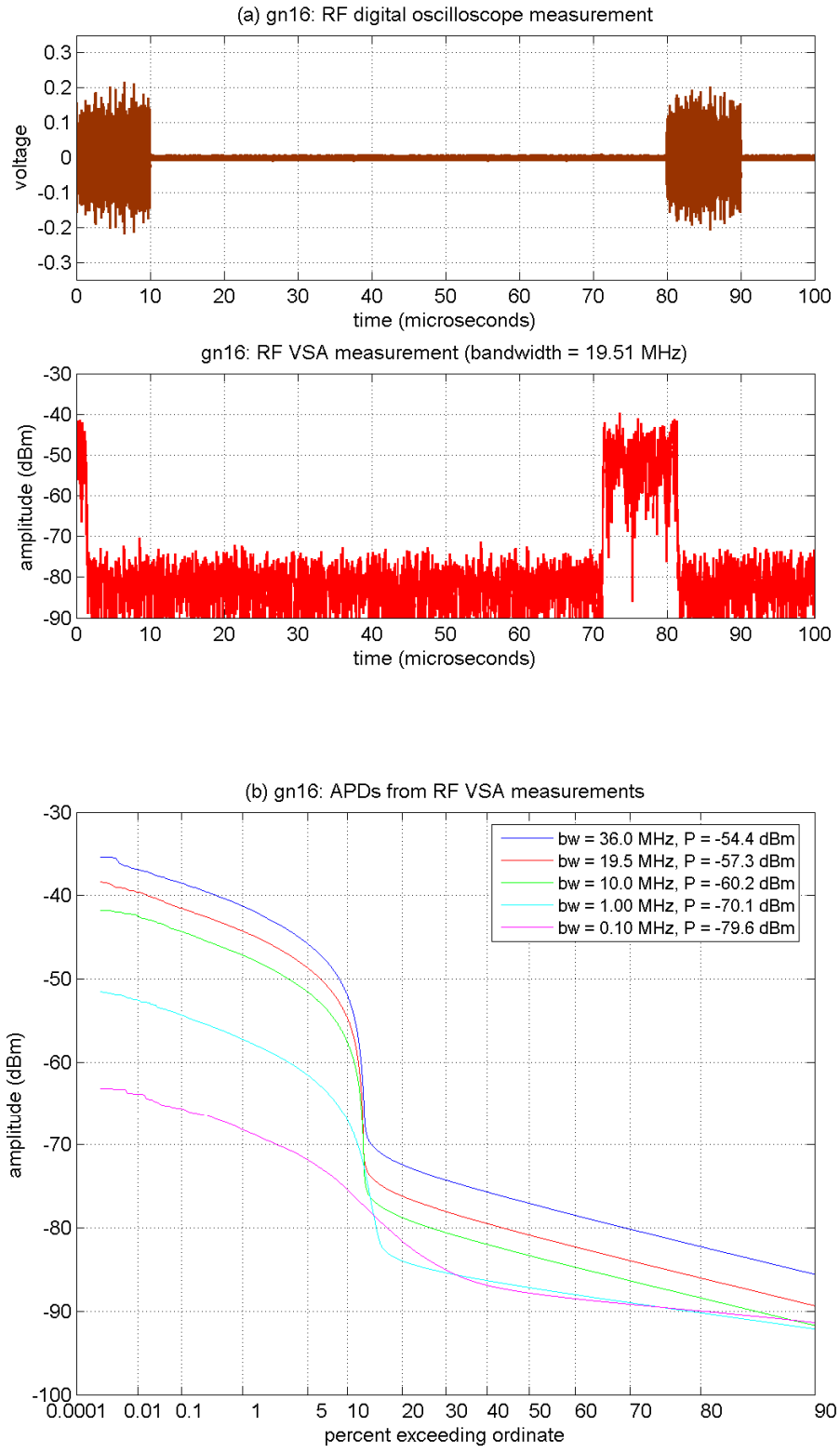

Figure D-33. RF measurements of GN-16 (τ_{on} = 10000 ns, ζ = 0.1250).

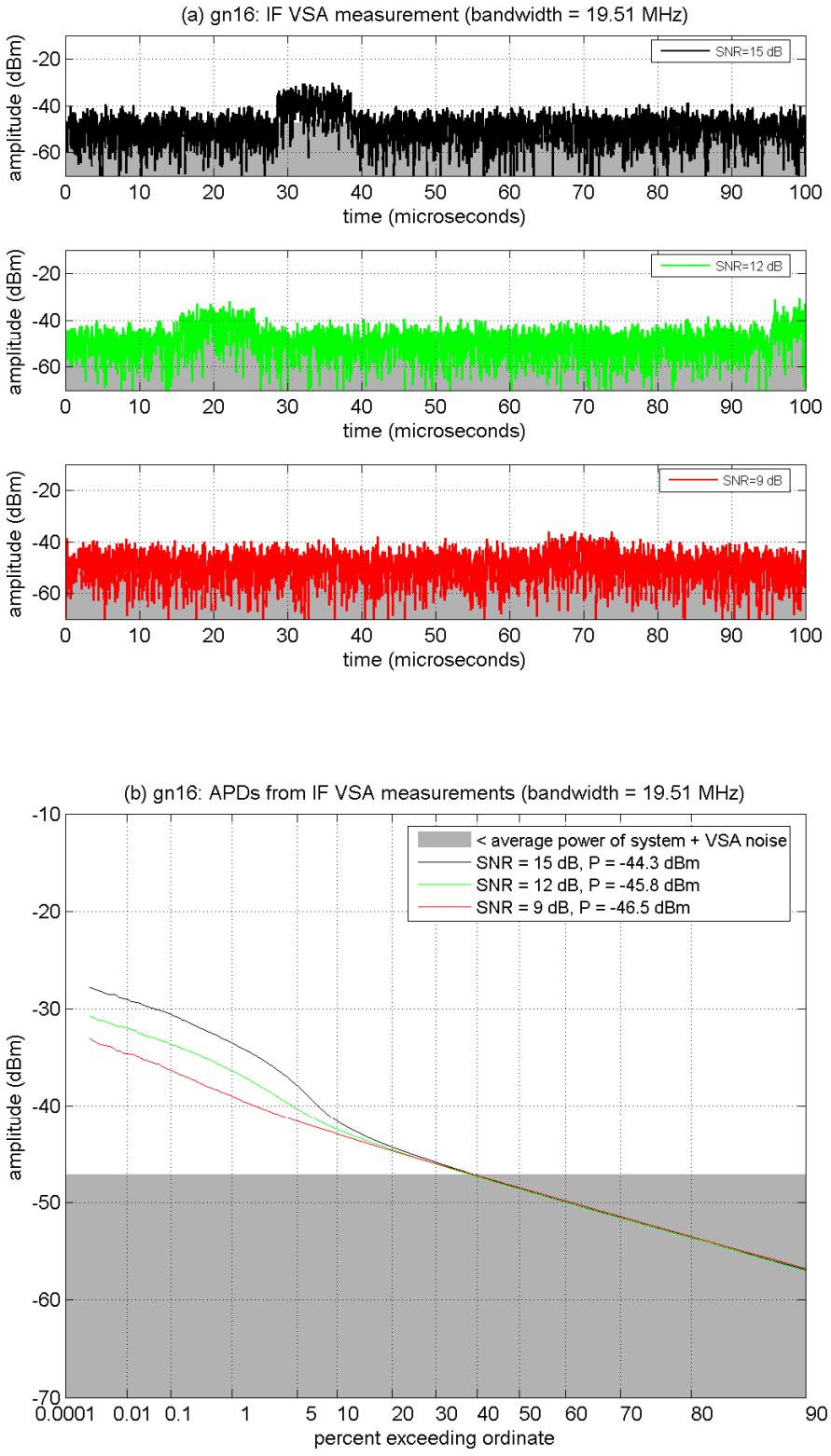

Figure D-34. IF measurements of GN-16 at INR_{TOV}.

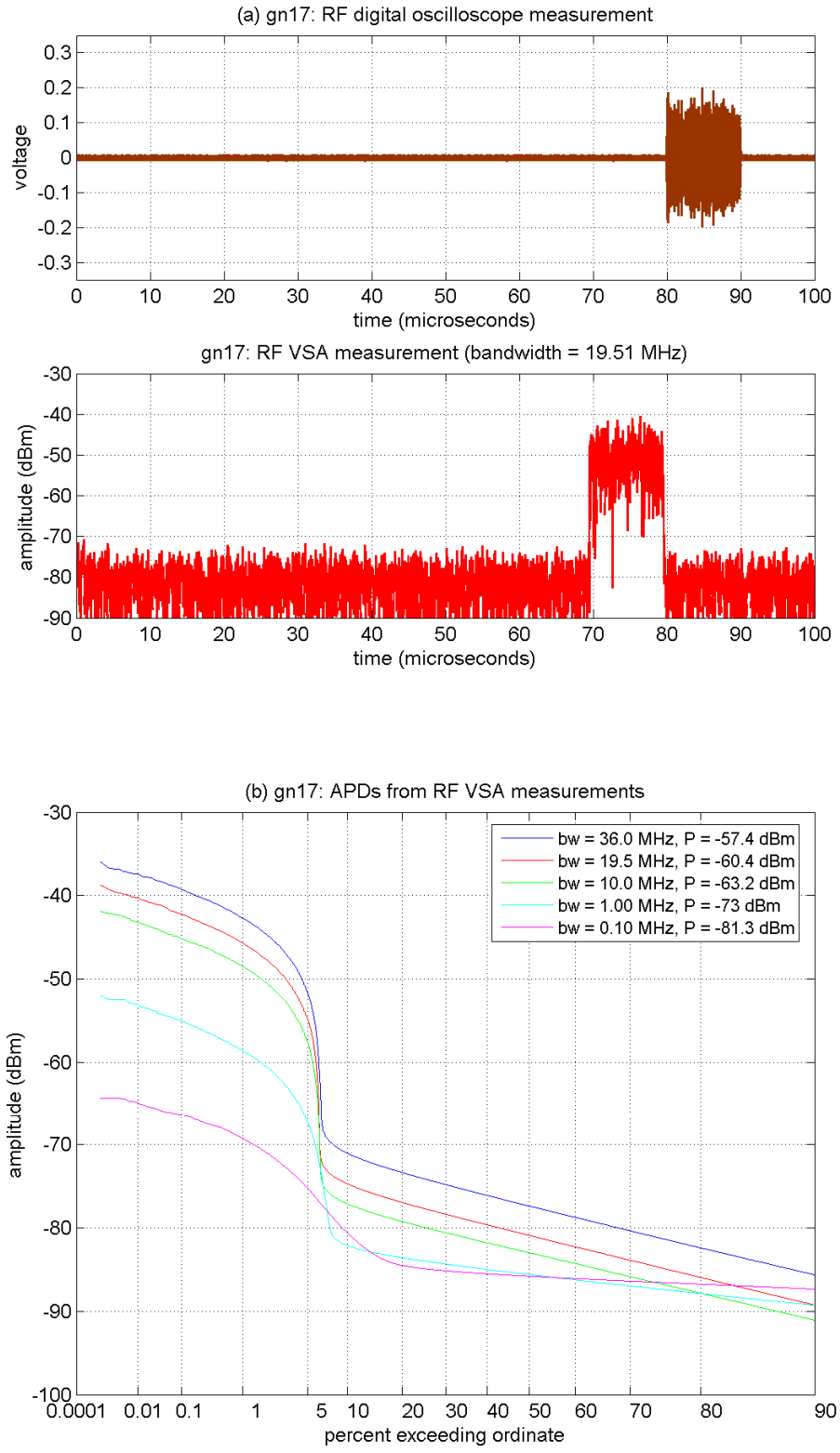

Figure D-35. RF measurements of GN-17 (τ_{on} = 10000 ns, ζ = 0.0625).

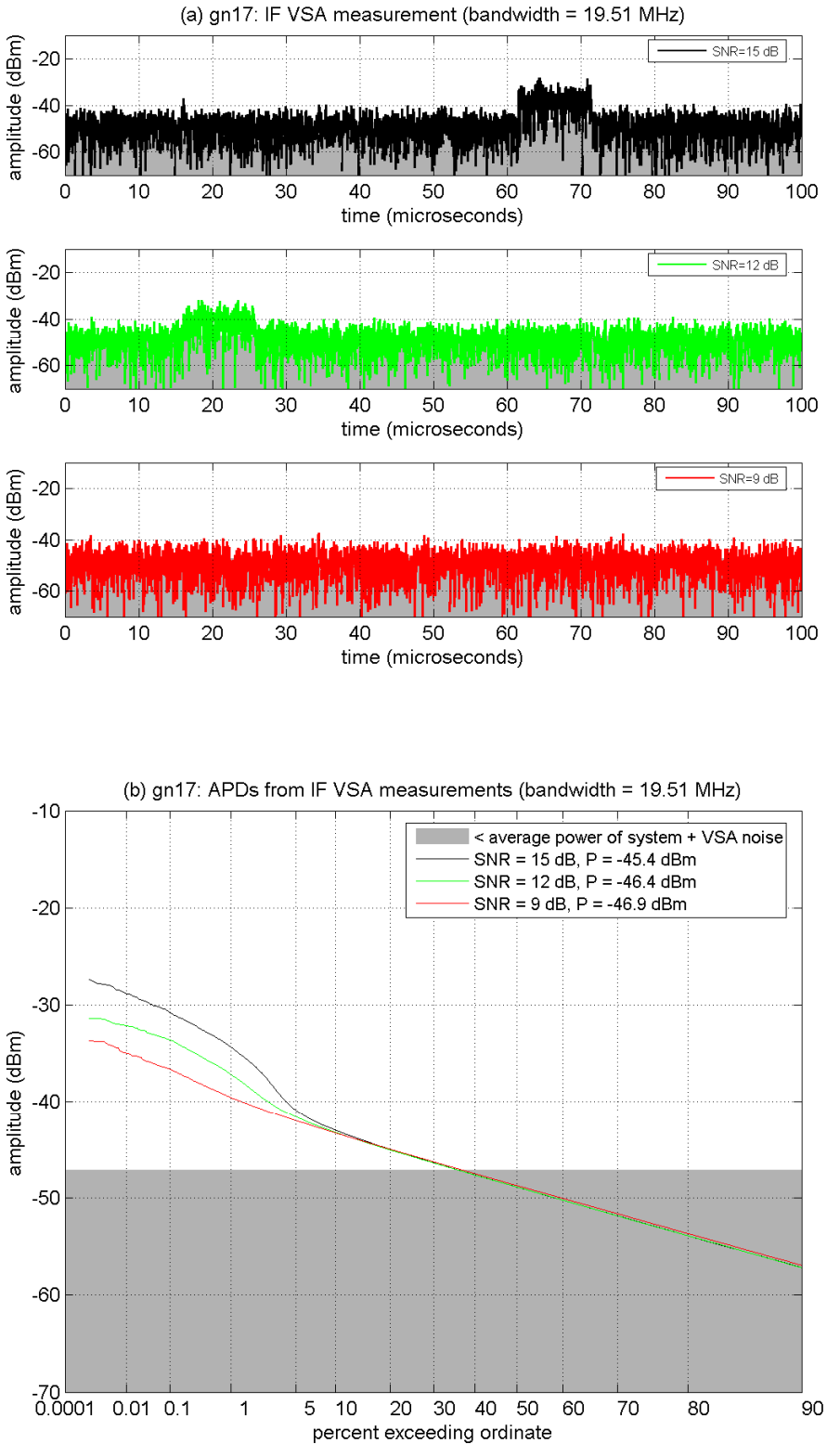

Figure D-36. IF measurements of GN-17 at INR_{TOV}.

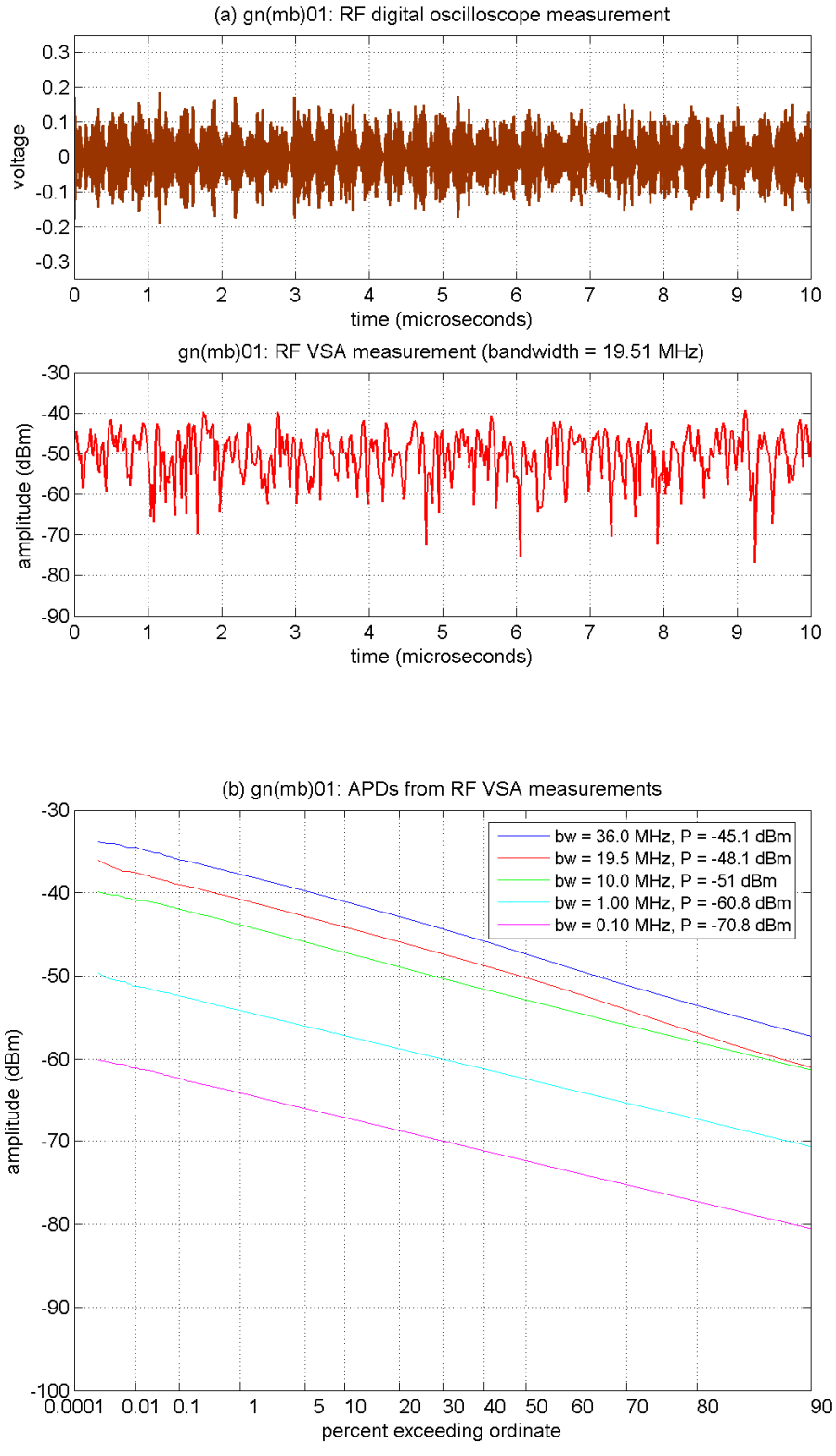

Figure D-37. RF measurements of GN(MB)-01 ($b = 1$, $d = 1$).

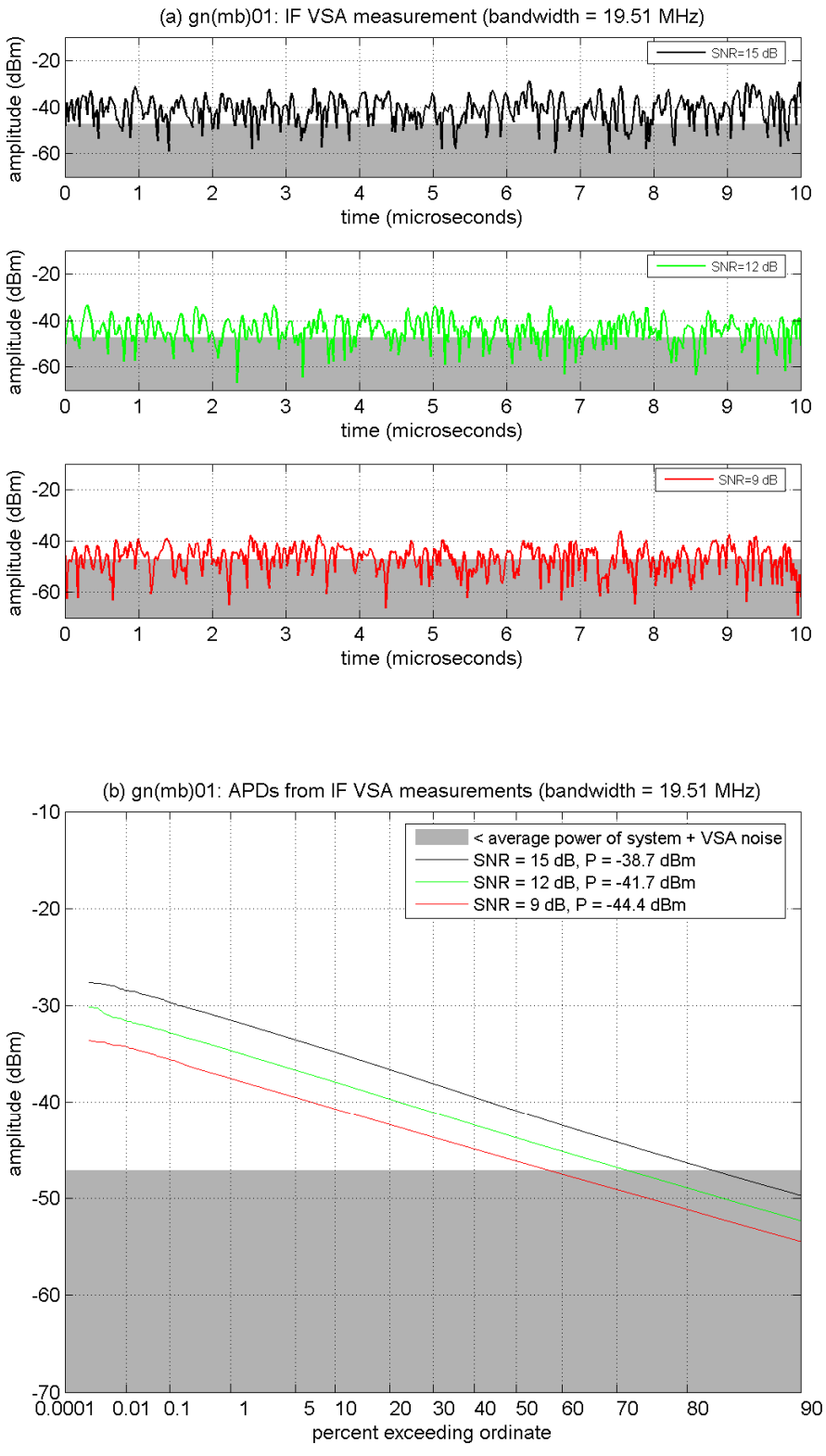

Figure D-38. IF measurements of GN(MB)-01 at INR_{TOV}.

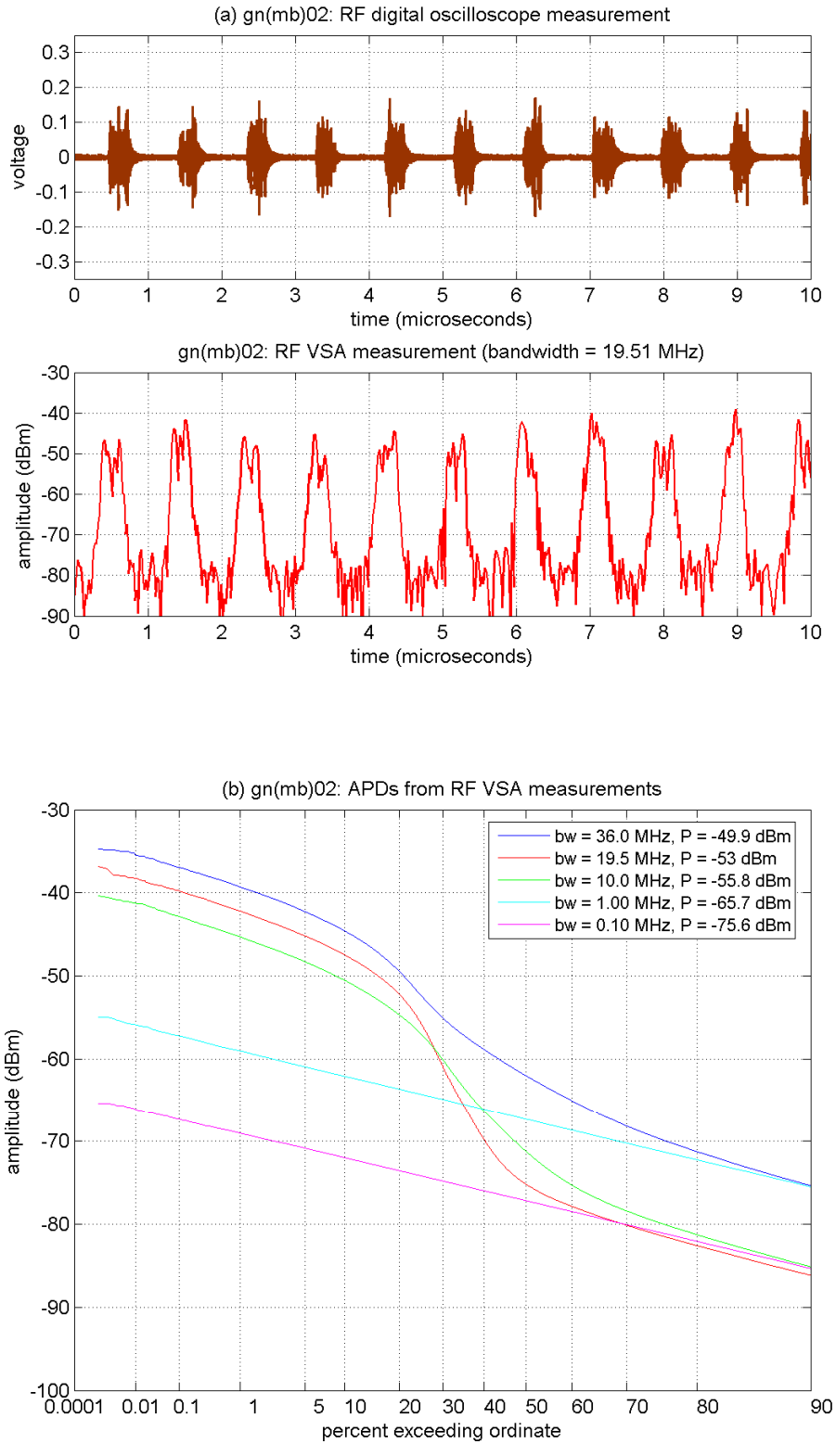

Figure D-39. RF measurements of GN(MB)-02 ($b = 3$, $d = 1$).

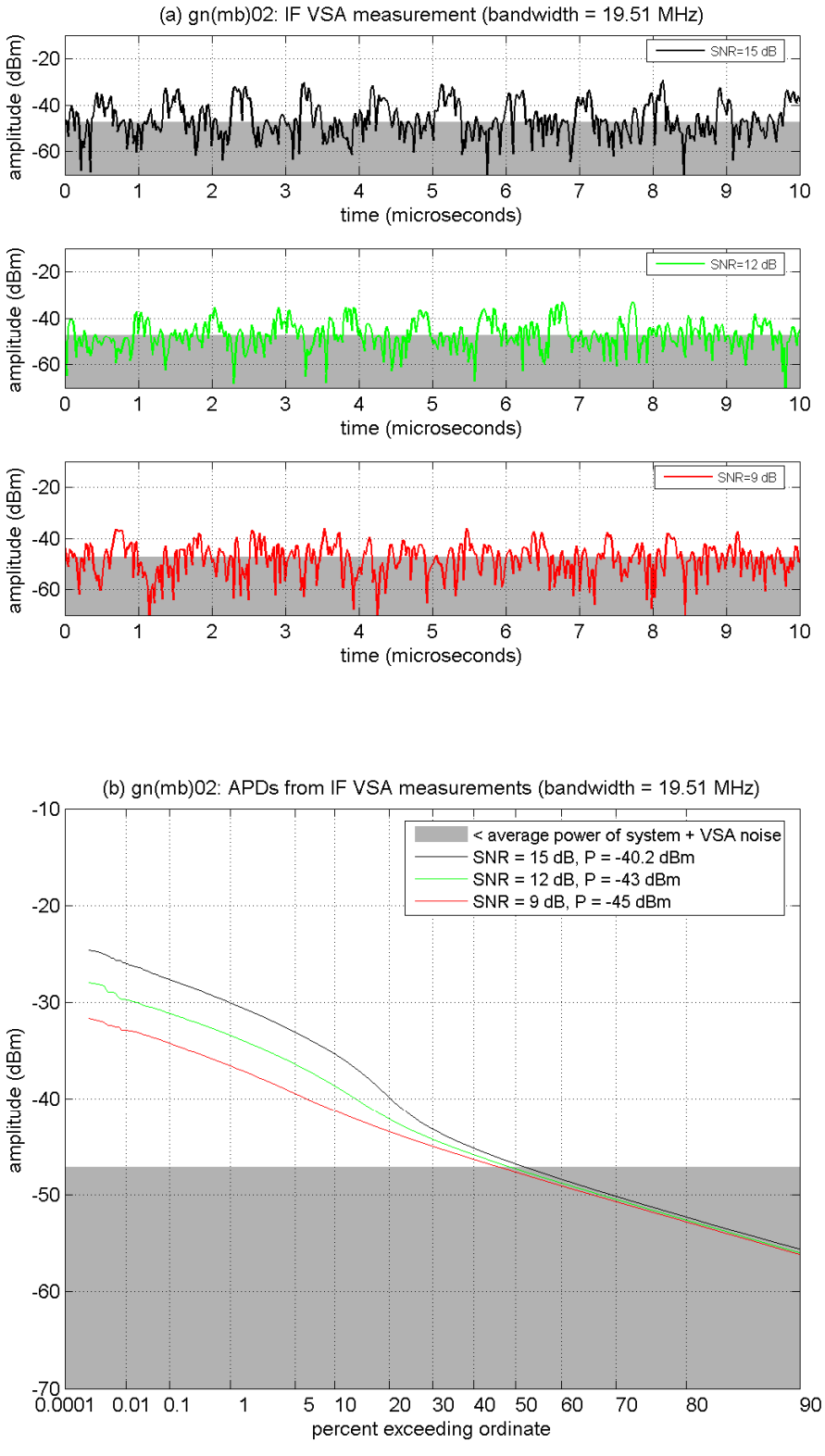

Figure D-40. IF measurements of GN(MB)-02 at INR_{TOV}.

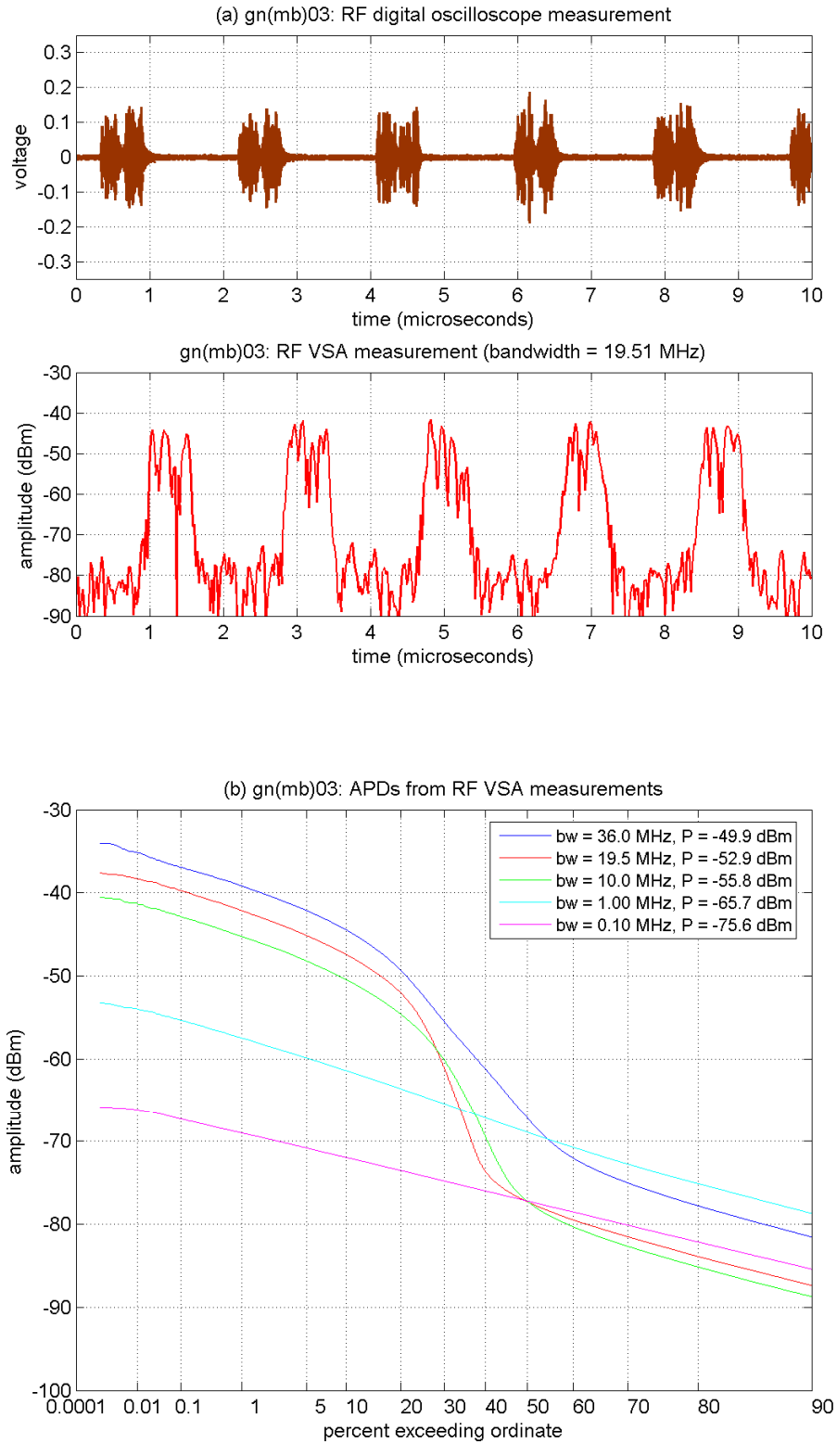

Figure D-41. RF measurements of GN(MB)-03 ($b = 3$, $d = 2$).

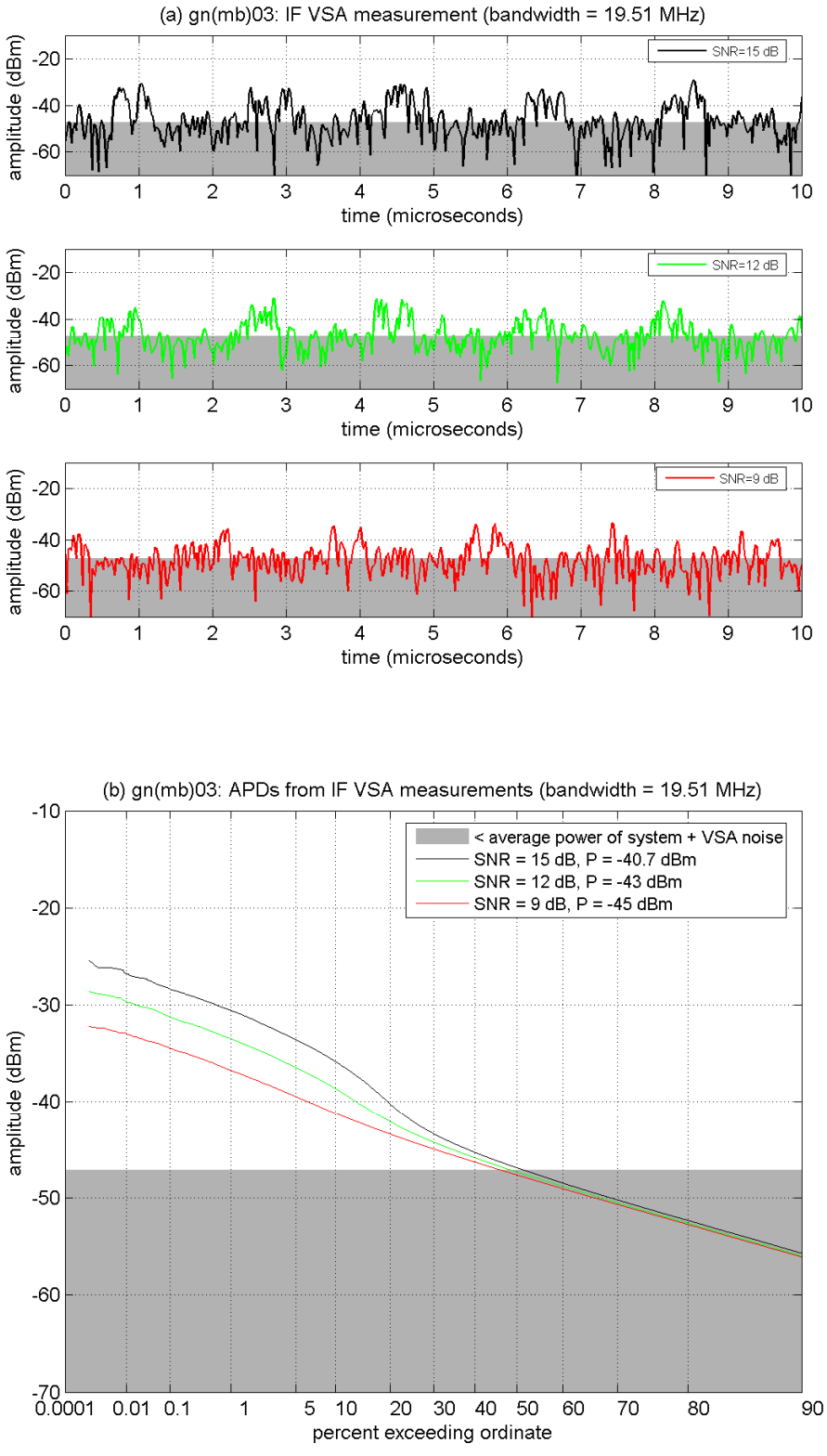

Figure D-42. IF measurements of GN(MB)-03 at INR_{TOV}.

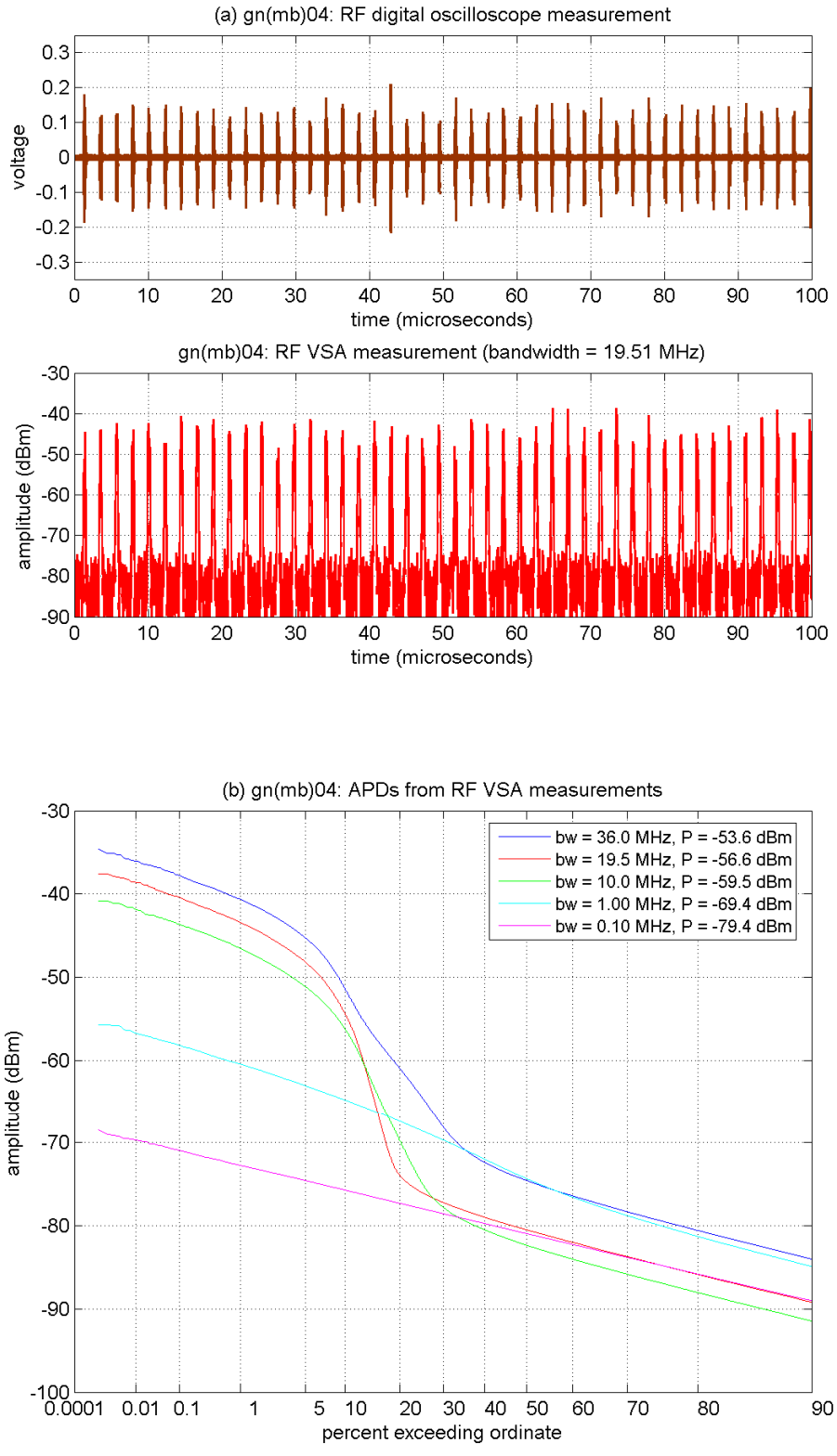

Figure D-43. RF measurements of GN(MB)-04 ($b = 7$, $d = 1$).

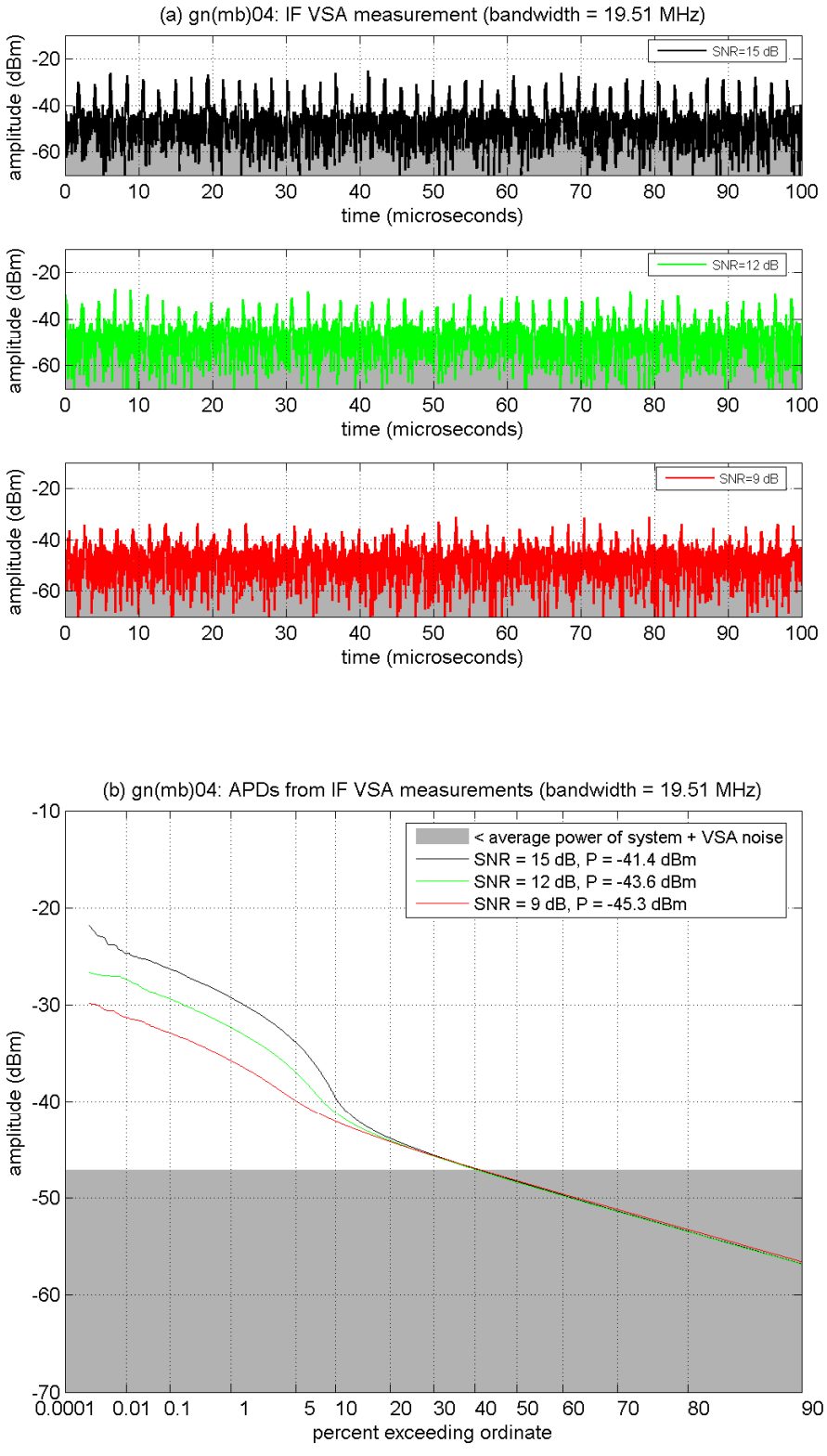

Figure D-44. IF measurements of GN(MB)-04 at INR_{TOV}.

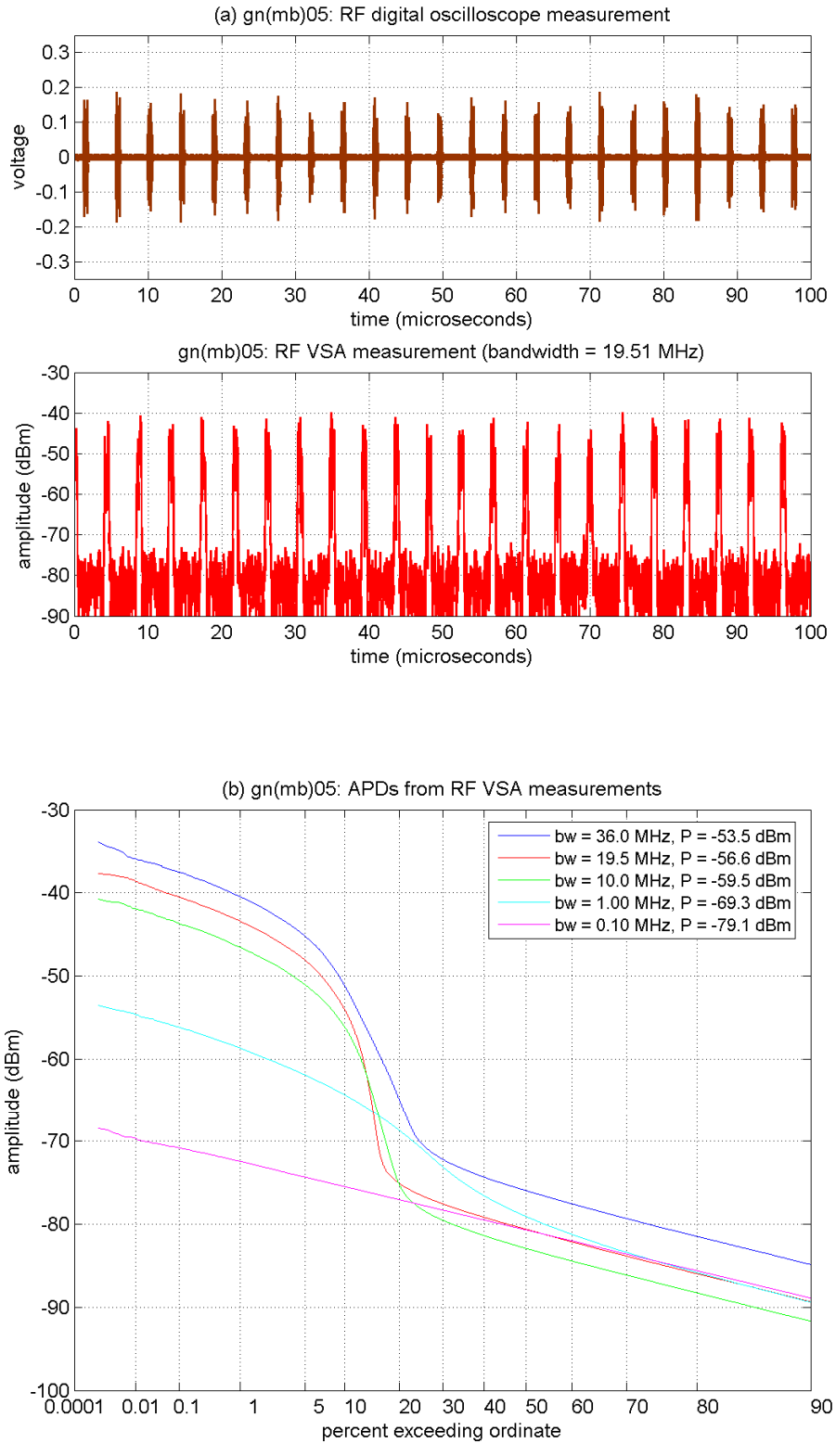

Figure D-45. RF measurements of GN(MB)-05 ($b = 7$, $d = 2$).

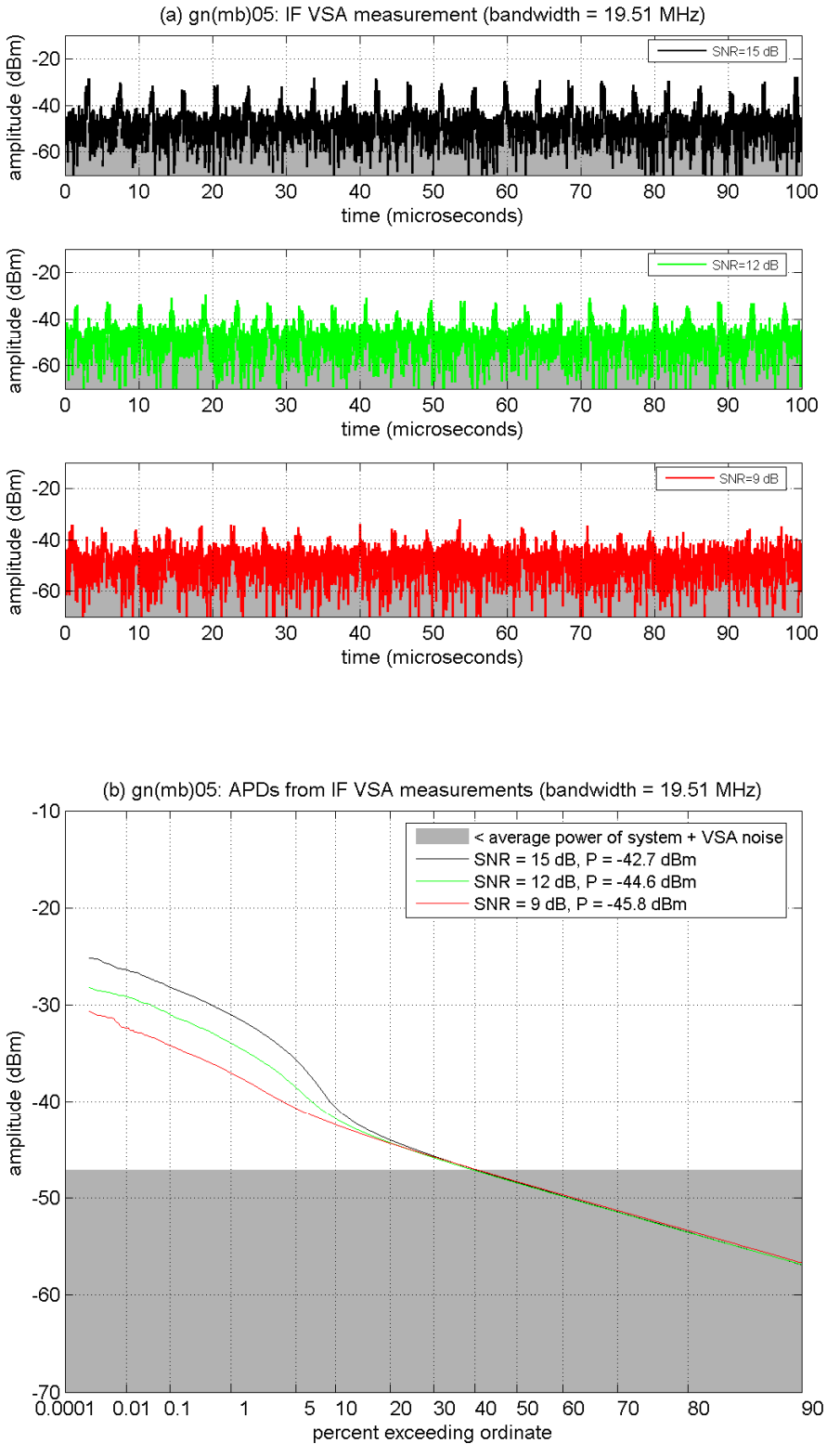

Figure D-46. IF measurements of GN(MB)-05 at INR_{TOV}.

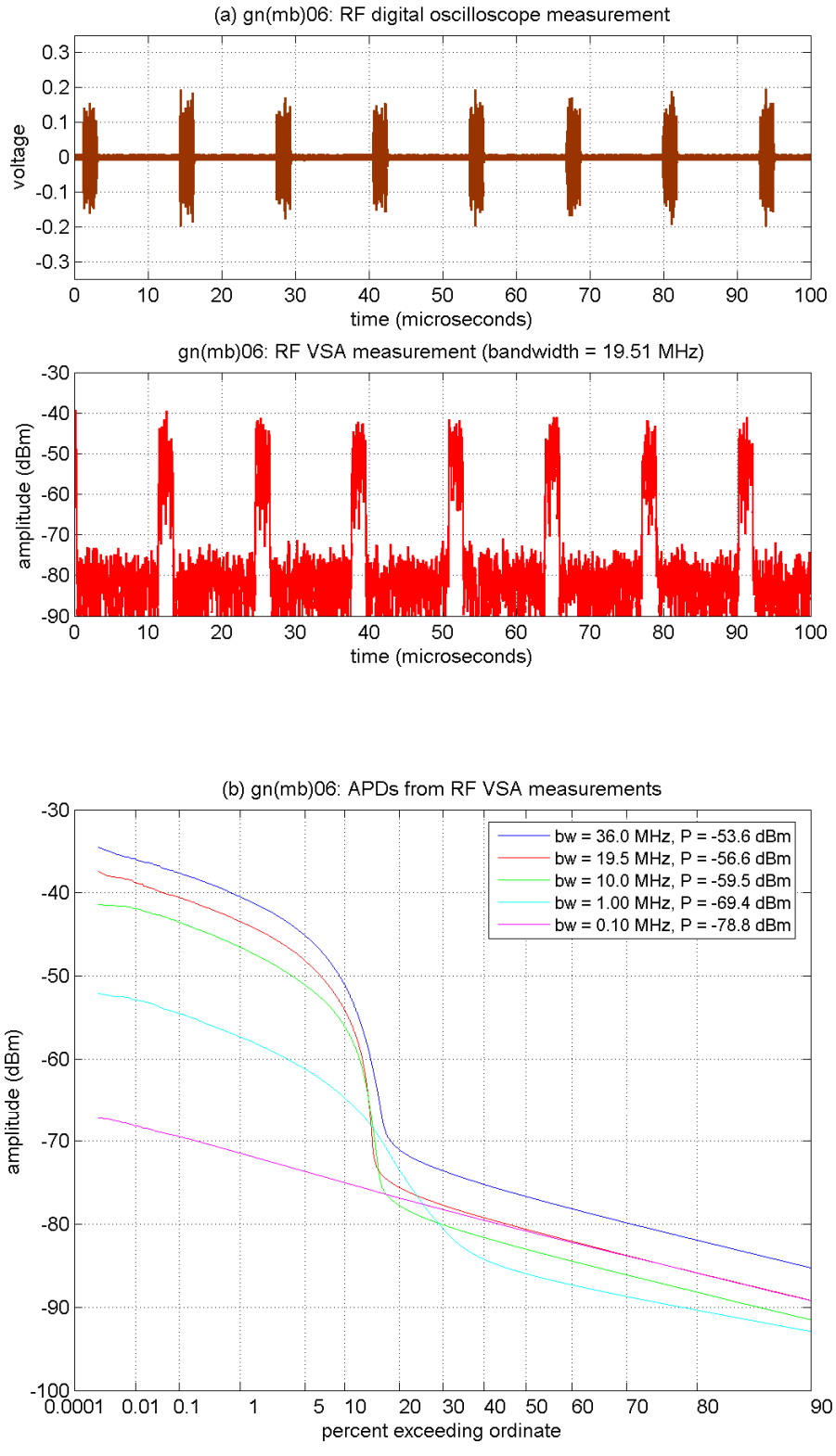

Figure D-47. RF measurements of GN(MB)-06 ($b = 7$, $d = 6$).

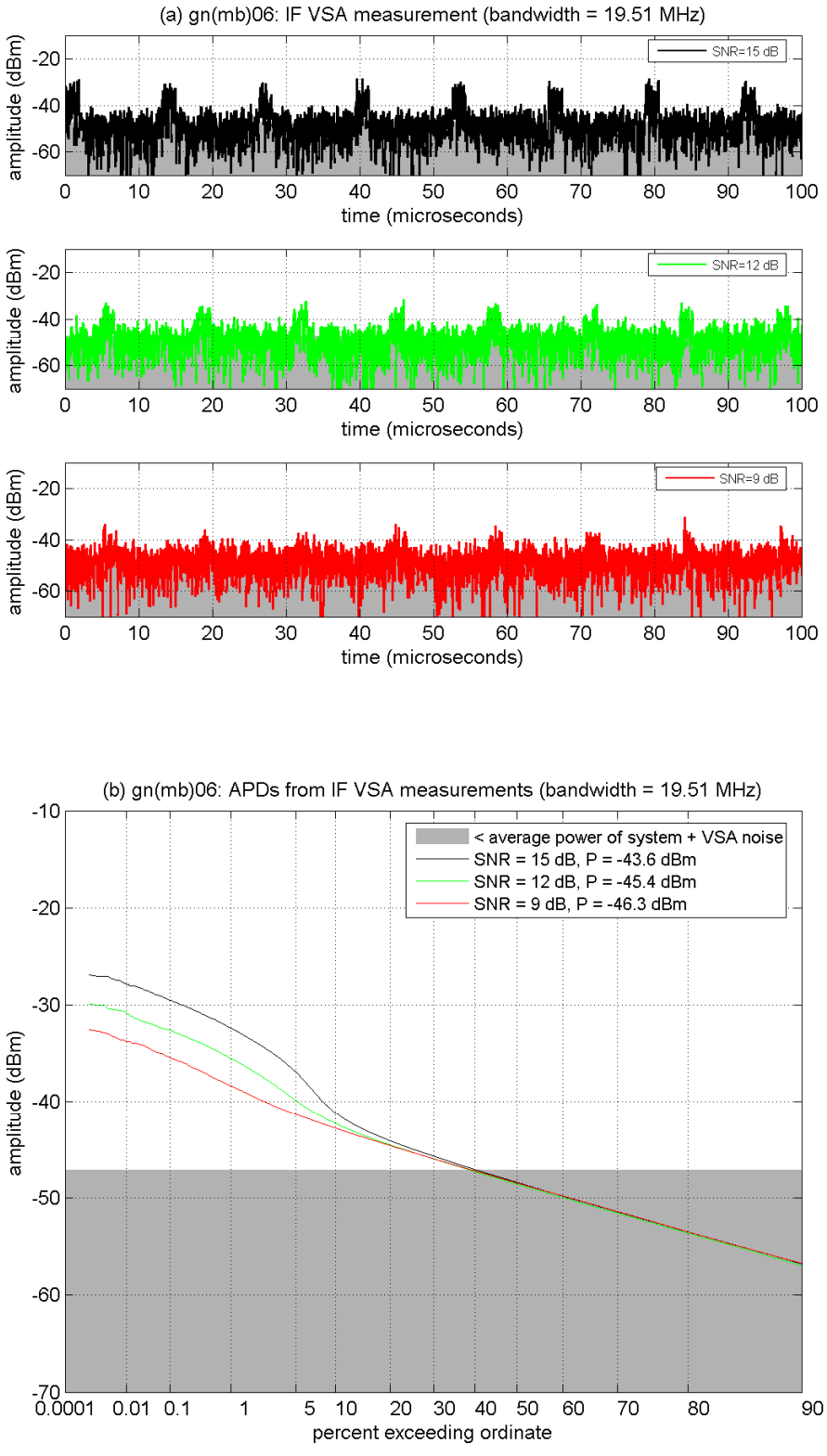

Figure D-48. IF measurements of GN(MB)-06 at INR_{TOV}.

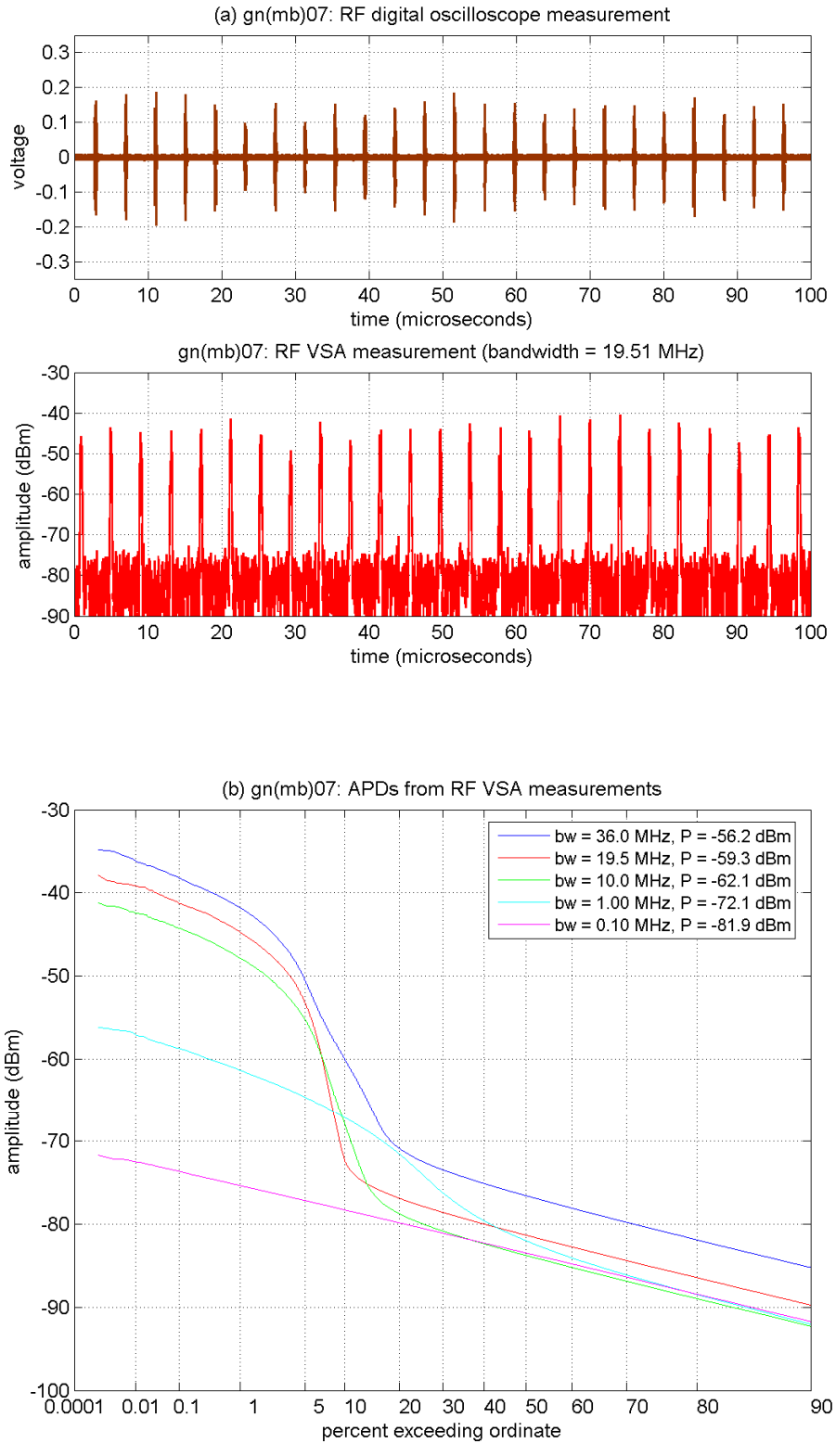

Figure D-49. RF measurements of GN(MB)-07 ($b = 13$, $d = 1$).

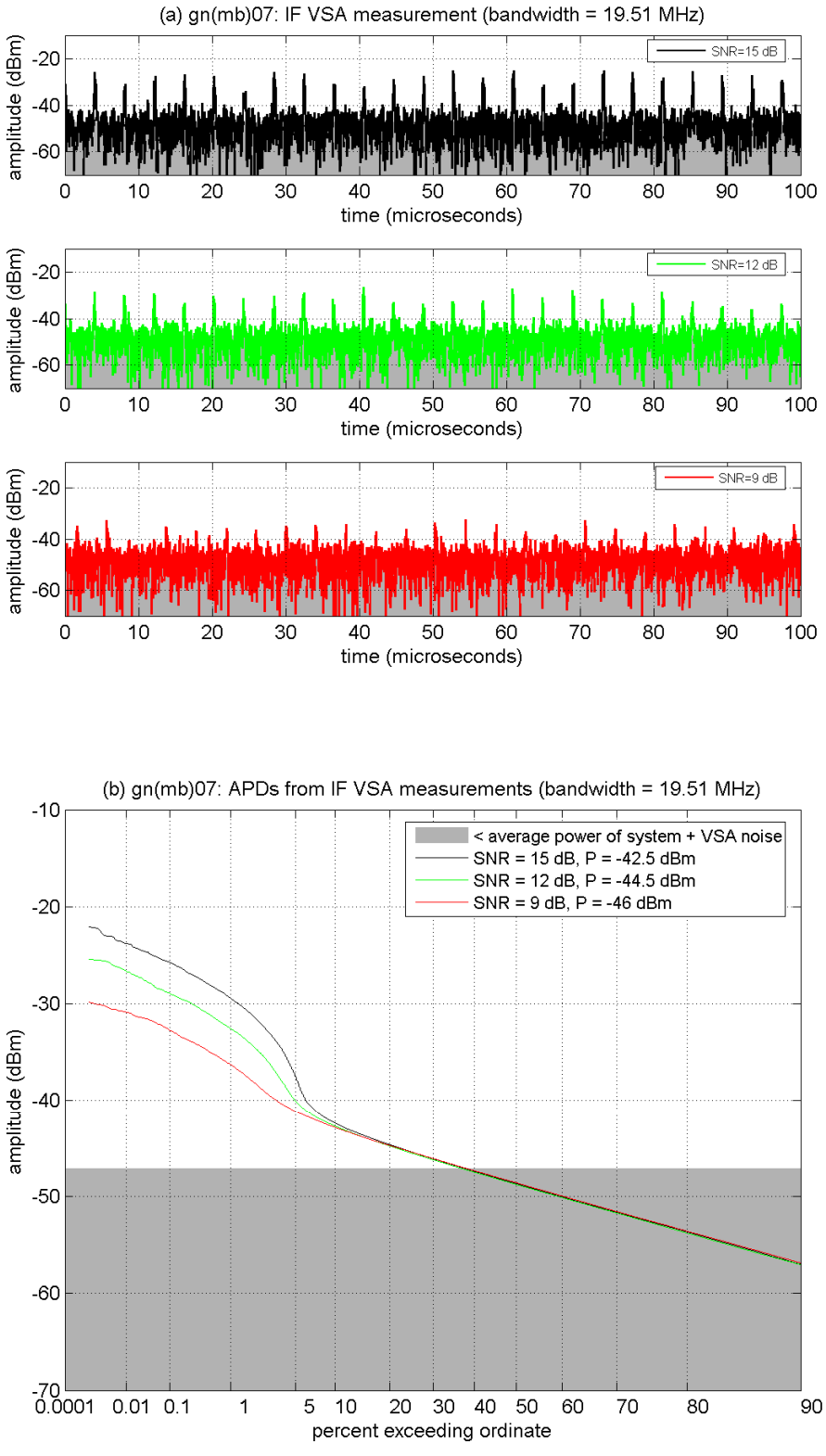

Figure D-50. IF measurements of GN(MB)-07 at INR_{TOV}.

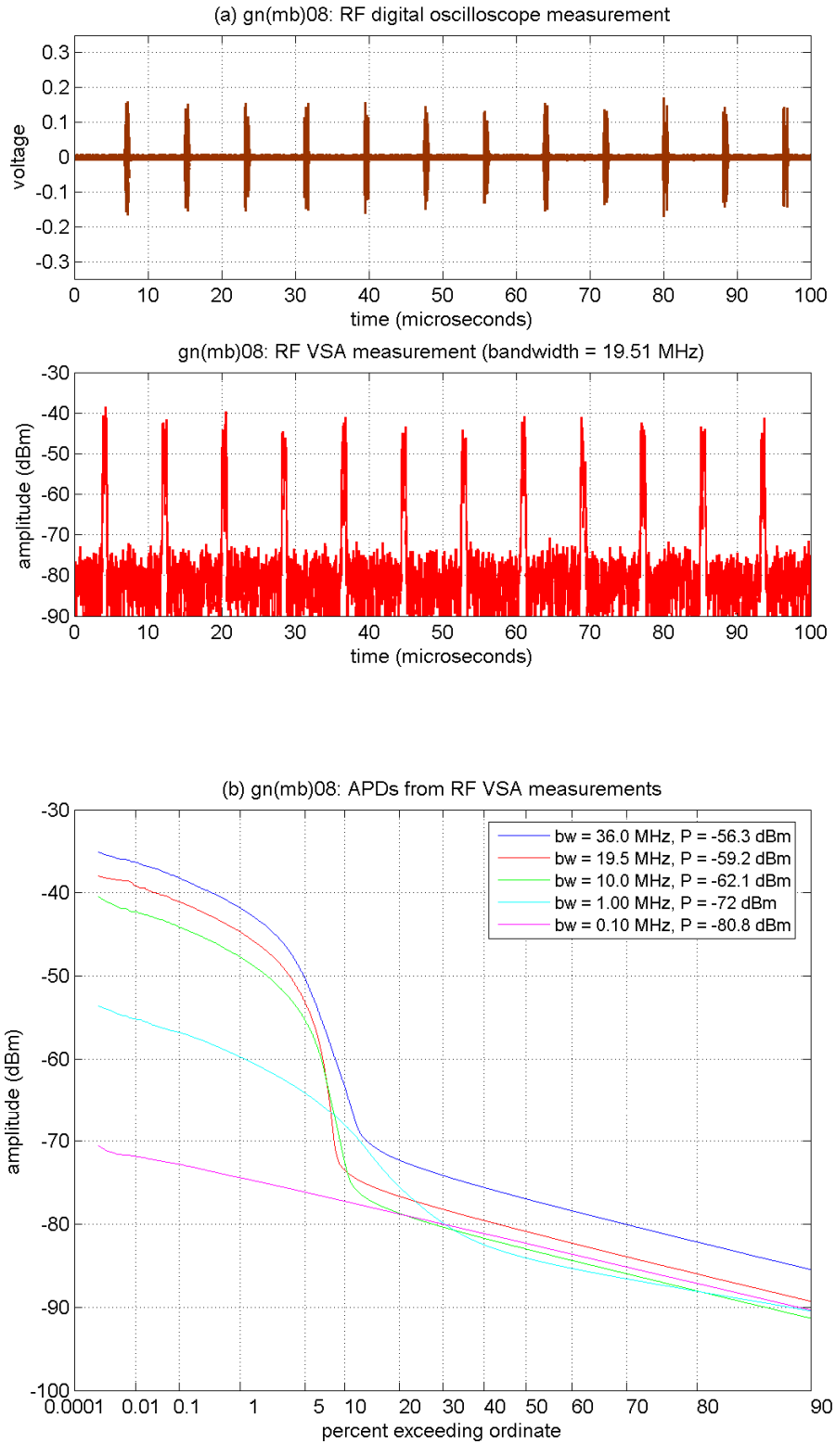

Figure D-51. RF measurements of GN(MB)-08 ($b = 13$, $d = 2$).

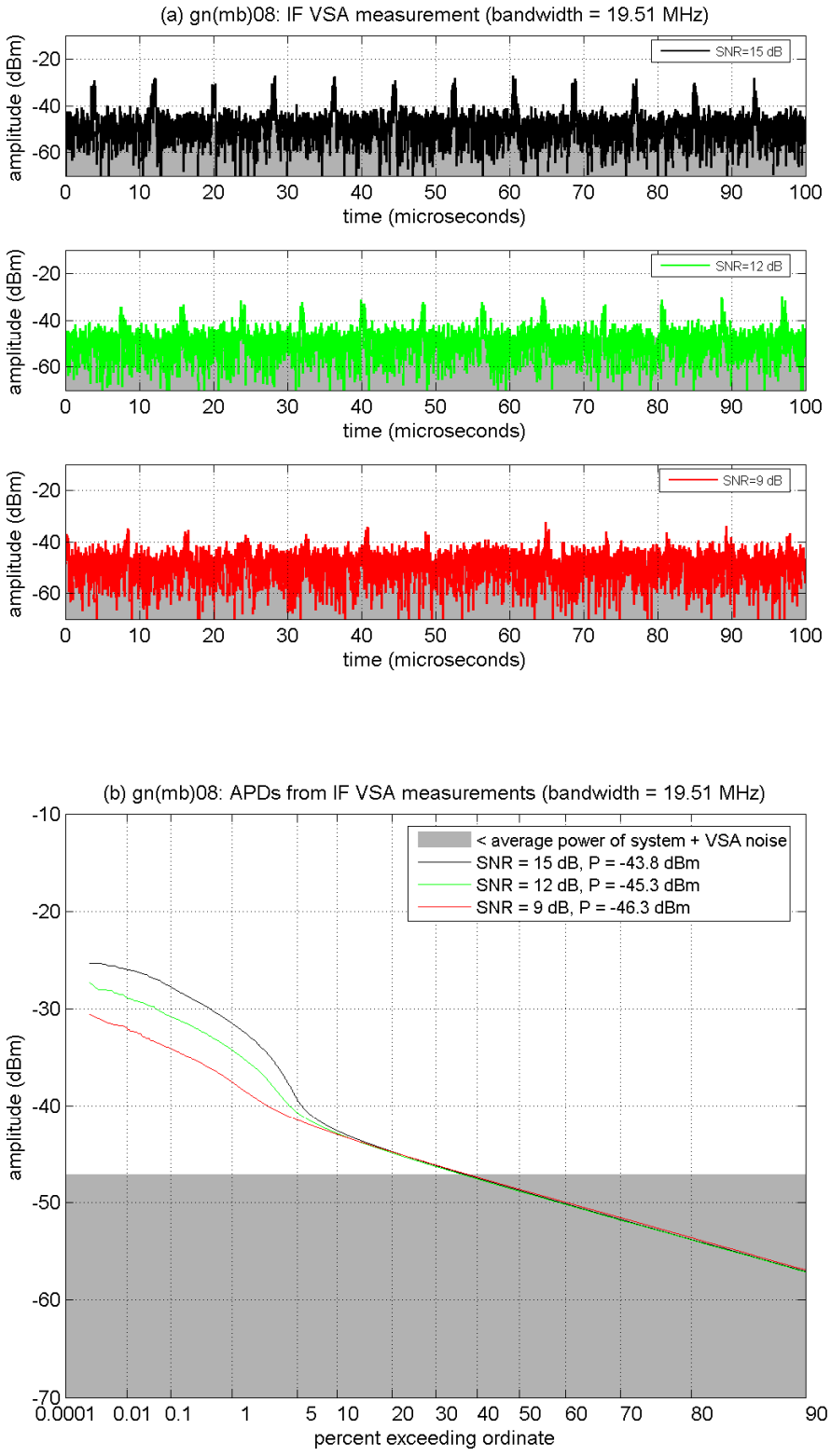

Figure D-52. IF measurements of GN(MB)-08 at INR_{TOV}.

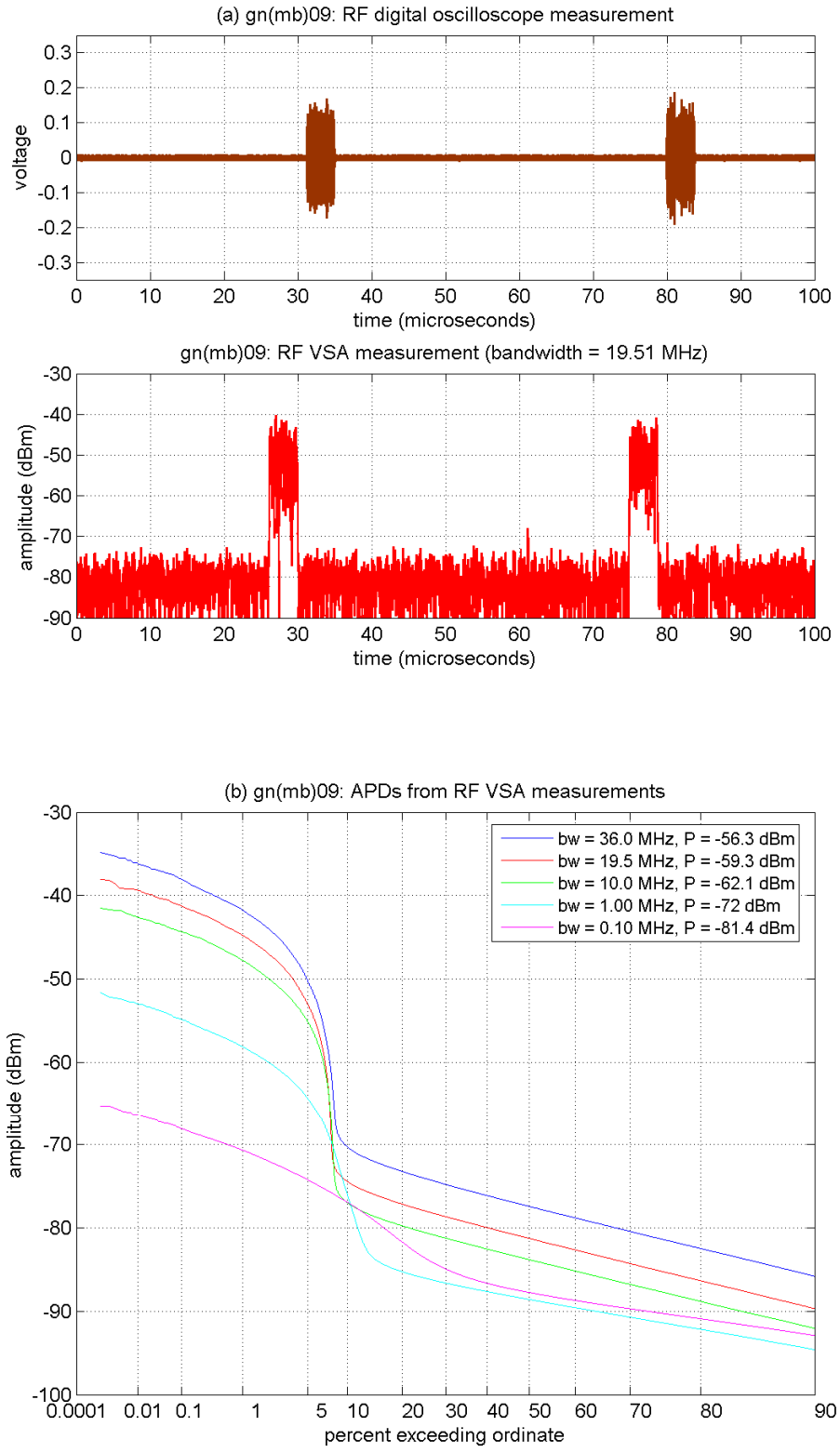

Figure D-53. RF measurements of GN(MB)-09 ($b = 13$, $d = 12$).

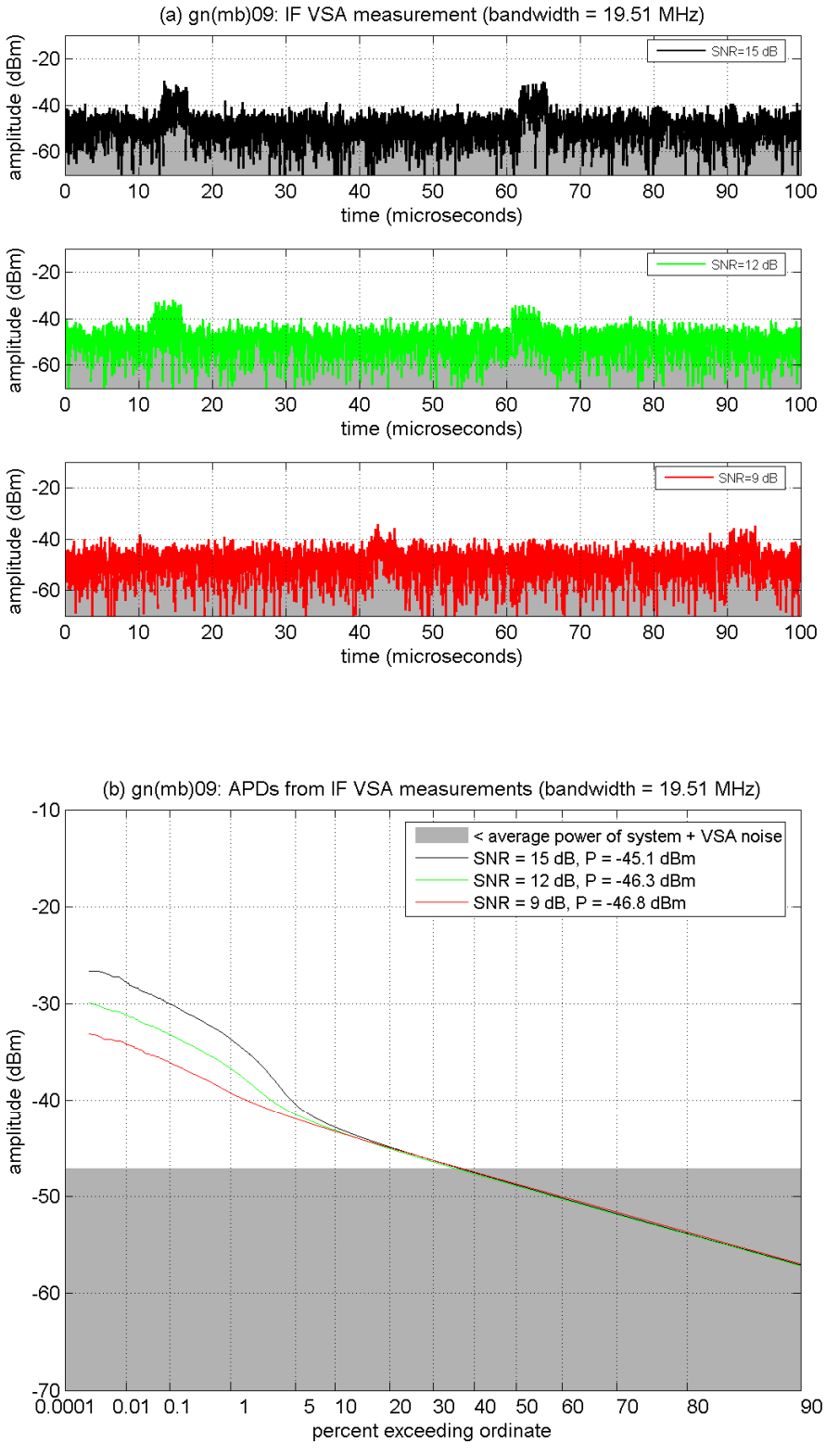

Figure D-54. IF measurements of GN(MB)-09 at INR_{TOV}.